Scientific report; WR 96-05

KNMI

Simulations of the response of the ocean waves in the North Atlantic and North Sea to CO_2 doubling in the atmosphere

Kathy M. Rider,
Gerbrand J. Komen and
Jules J. Beersma

De Bilt, 1996

Scientific report = wetenschappelijk rapport; WR 96-05

De Bilt, 1996

P.O. Box 201
3730 AE De Bilt
Wilhelminalaan 10
Telefoon 030-220 69 11
telefax 030-221 04 07

Auteurs: Kathy M. Rider,
Gerbrand J. Komen and
Jules J. Beersma

UDC: 551.556.8
551.521.32
551.466.3
551.583

ISSN: 0169-1651

ISBN: 90-369-2109-0

© KNMI, De Bilt. Niets uit deze uitgave mag worden verveelvoudigd en/of openbaar gemaakt worden door middel van druk, fotocopie, microfilm, of op welke wijze dan ook, zonder voorafgaande schriftelijke toestemming van het KNMI.

● ● ● ●

Simulations of the response of the ocean waves in the North Atlantic and North Sea to CO_2 doubling in the atmosphere

Kathy M. Rider, Gerbrand J. Komen and Jules J. Beersma

Royal Netherlands Meteorological Institute (KNMI),
P.O. Box 201, 3730 AE De Bilt, The Netherlands

August 1996

Abstract

Data from high resolution numerical experiments are analysed to study the effect of greenhouse warming on the atmospheric climatology of the North Atlantic region. By comparing data from a control experiment with analysis data, it is shown that the climate model simulates a fairly realistic current climate. A $2xCO_2$ experiment is compared with the control experiment. In this comparison, the mean sea level pressure, the near surface winds and the variability of the 500 hPa geopotential heights are considered. The spatial distribution and frequency of the storms over the North Atlantic are also studied. Small regional differences are detected. In particular, there is an increase in the frequency of winds from the northwesterly direction. However, these effects are small compared to the magnitude of the low frequency natural variability in the North Atlantic area. It is therefore not possible to say whether they are caused by external forcing.

Near-surface winds from the two climate model data sets were used to drive an ocean wave model, WAM, in order to determine the sensitivity of the wave climatology to the small differences seen in the climatology of the winds. The average wave heights, the variability of the wave heights and the extreme wave heights of the two simulations are compared. Further analysis of the extreme wave heights is done using statistical techniques. Small local differences are detected which reflect the differences in the wind fields from the climate model experiments, although their relative magnitude is generally smaller than that of the anomalies in the winds.

Contents

1 Introduction

Recent studies claim there is evidence of an increase in the intensity and the frequency of extra-tropical storms (Dronia, 1991; Schinke, 1993; Stein and Hense, 1994). Bacon and Carter (1991), Hogben (1994) and van Hooff(1993) find positive trends in the observed significant wave heights in the northeastern Atlantic and adjacent seas. These claims alone have serious implications for the off-shore oil industry, fisheries, shipping companies, insurance companies and coastal engineers. However, what is causing more concern amongst these groups, is that the positive trends in storms and waves have been linked, by articles in the public press, to the increase in the greenhouse gases in the atmosphere. The implication being that, as atmospheric levels of CO_2 concentrations rise, storminess and wave heights in the North Atlantic region will continue to increase into the next century.

Others, however, do not agree that there is any strong evidence at all for increasing trends in the storm or wave climate over the North Atlantic. Kaas (1996) suggests that studies which do show such positive trends have analysed data sets that are of too short a period to fully capture the natural variability of the circulation in this area. There is also some doubt about the homogeneity of data sets used in some studies (Nicholls et al., 1996; Schmidt and von Storch, 1993). Using long homogeneous time series of observations, it has been shown that the frequency of extreme storms in the southeastern North Sea has not changed in the past 100 years (Schmidt and von Storch, 1993). Similarly, von Storch et al. (1993) have shown that there is little trend in the number of storm days in Iceland and no trend in the frequency of extreme surge heights at Hoek van Holland in the Netherlands.

Not only is there disagreement about current trends in the storm and wave climates based on observations and model analyses, but there is also little agreement between models on the effects of increased concentrations of greenhouse gases on mid-latitude storms (Beersma, 1994; Collier et al., 1994; and Kattenberg et al., 1996). In particular, the net effect of the predicted decrease in the pole-to-equator temperature gradient at the surface and the competing increase in the pole-to-equator temperature gradient in the stratosphere has yet to be adequately estimated (Held, 1993). For example, while Hall et al. (1994) found an intensification and a poleward shift of the Northern Hemisphere storm tracks in the high resolution United Kingdom Meteorological Office slab model, Lambert (1995), using the Canadian Centre for Climate slab model, found no such shift and found a slight shortening of the Atlantic tracks which would indicate a reduction in storm activity.

In response to the growing uncertainty with respect to storminess and the height of waves in the North Atlantic and North Sea area, the WASA project, was established (WASA group, 1995). The objectives of this project were to verify whether storms in the North Atlantic region have become more frequent and more intense over the course of this century, to

investigate possible future changes in the storm climate, and to determine the response of the surge and wave statistics to these changes. To accomplish these objectives, the participants of the WASA project have worked together to reconstruct the storm, surge and wave climates in the North Atlantic region for a large part of the 20th century, and to construct a possible scenario for the 21st century. This was done by analysing long homogeneous data sets of local parameters such as geostrophic winds, pressure tendencies and coastal water levels (Alexanderson et al., 1997; Bijl et al., 1997; Schmith and Kaas, 1997; and von Storch et al., 1997), analysing waves hindcast for a 40-year period using a third generation wave model, WAM Cycle 4, (Lozano et al., 1997a; and Lozano et al., 1997b), and analysing data extracted from ship routing charts (Bouws et al., 1996). Also, data from two high resolution climate model experiments, a control and a $2xCO_2$ scenario, have been analysed (Beersma et al.,1996). Using data from these experiments, the response of the surge climate to the climate change scenario has been simulated and analysed (Flather and Smith, 1997) and, finally, wave simulations, carried out using the WAM model, have been analysed.

This report is primarily concerned with the last item in the above list. The analysis of the 5-year wave simulations for the current atmospheric climate and for a possible future scenario are presented. We considered it useful to include an analysis of the climate model experiments, each consisting of just over five years of data, from which the winds were used to run the wave simulations. In doing this, we repeat some of the results presented in Beersma et al. (1996), but the analysis in this report is more detailed. Specifically, we make a more thorough analysis of the wind climatologies.

In sections 2 and 3 of this report we describe the set-up of the climate model experiments and the wave model simulations respectively. In section 4, we discuss the natural variability of the atmosphere over the North Atlantic and northwest Europe.

Section 5 addresses the question: is the control model climate a good approximation of the current climate? To ascertain this we make comparisons with ECMWF analyses. In particular, we analyse the mean sea level pressure (MSLP), the near surface (10 m) winds, the variability of the 500 hPa height, the frequency and distribution of storms over the North Atlantic for the 6 winters available from the control experiment.

After having established that the atmospheric circulation of the control experiment is consistent with the current climate, we assess the effect of increased concentrations of atmospheric CO_2 on the atmospheric climatology in section 6.

The local differences that are identified between the control and the $2xCO_2$ experiment are rather small relative to the natural variability of the atmosphere. It was nevertheless considered useful to simulate the waves using the wind and ice fields from the climate model

runs. One reason for doing this is that we now have a reference data set of wave model output, both integrated parameters and wave spectra, which are available for use in future projects. We also wanted to determine how the small differences in the wind climatology influenced the wave climatology.

In section 7 the wave climatology of the control simulation is evaluated and verified using wave data from a 40-year hindcast data set prepared by Lozano et al. (1997a), and with analysed wave data extracted from KNMI ship routing charts (Bouws et al, 1996). To do this, we analyse the total significant wave height field. This parameter is the wave height resulting from both wind sea energy and swell energy, hence 'total', and it is the quantity traditionally estimated when observing the sea state, hence 'significant'.

We examine the anomalies in the waves of the $2xCO_2$ simulation in section 8. Section 9 summarises the results presented in this report and in section 10 some conclusions are given.

2 Description of the set-up of the climate model time slice experiments

Two climate model experiments are analysed in this report: a control and a $2xCO_2$ scenario. They each consist of just over five years of atmospheric fields produced by integrating an atmospheric general circulation model (AGCM) in uncoupled mode. The model used was the ECHAM3 spectral model with 19 levels and a horizontal resolution of T106 (triangular truncation at total wave number 106) at the model levels and N80 (80 grid points between each pole and the equator) at the surface.

Conventional climate model experiments are carried out by integrating a coupled ocean-atmosphere model over several decades. However, if a high resolution AGCM is to be used, this method becomes prohibitively expensive in terms of computer resources. Therefore, a method was devised whereby a high resolution AGCM is run in uncoupled mode for a relatively short period with prescribed boundary conditions, i.e. SSTs and sea-ice limits. These boundary conditions are obtained either from observations, in the case of a control, or from a lower resolution $2xCO_2$ climate run. The boundary conditions are updated once per month without any interannual fluctuations. In this way, high resolution data for a climate scenario can be simulated relatively inexpensively. This is usually referred to as a time slice experiment.

The control time slice experiment analysed in this report was produced by integrating the ECHAM3 model (T106 resolution) for just over five years using boundary conditions specified according to the observed (1979-1988) climatology.

For the $2xCO_2$ time slice experiment, SSTs from an earlier experiment by Cubasch et al. (1992) were used. In this experiment, the effect of increased atmospheric CO_2 concentrations were studied with a coupled ocean-atmosphere model. The atmospheric component of the coupled model was ECHAM1 with horizontal resolution T21 and the ocean component was the Large Scale Geostrophic (LSG) ocean model. These simulations included a control and a run in which the coupled model was integrated over a 100-year period under the assumption of a monotonous increase in CO_2 concentration (about 1% per year), in agreement with the IPCC Scenario A. The boundary conditions for the high resolution AGCM run were then calculated by adding the anomalies of the coupled run at the time of CO_2 doubling (after about 60 years of integration) to the observed (1979-1988) climatology. Using these boundary conditions, the ECHAM3 model (T106 resolution) was integrated for just over five years.

3 Description of the set-up of the wave model simulations

A third generation wave model, WAM Cycle 4 (Komen et al., 1994), was used to simulate waves with the wind forcing and ice limits extracted from the two time slice experiments which are described in the previous section. The model was run on two nested grids, a coarse grid (North Atlantic and adjacent seas) and a fine grid (Northeast Atlantic and adjacent seas), see figure 1a. The boundary conditions of the fine grid are obtained from the coarse grid points which coincide with the boundary of the fine grid. At these points energy is transferred into the fine grid. The fine grid simulation was a shallow water run, i.e. there is bottom dissipation, and the depth refraction was switched on, while the coarse grid simulation was a deep water run with no depth refraction.

The wind fields were interpolated from an N80 Gaussian grid to a lat/lon grid with resolution 1.5 x 1.5 degrees for the coarse grid area and 0.75 x 0.5 degrees for the fine grid area. And they were interpolated in time from twice daily to four times per day. The sea-ice limits from the climate model experiments were also interpolated to the two different grid resolutions. The wave model was set up to read each new field of sea-ice limits at the beginning of each month (Lozano et al., 1997a). Sea-ice grid points are interpreted by the model as land points: these points have zero wave energy at all times.

The wave model output consists of wave energy spectra for all grid points every three hours and 23 integrated parameters every three hours. For more details see Rider (1996).

4 Low frequency atmospheric variability over the North Atlantic

When evaluating a future climate scenario we need to be able to distinguish between a signal due to low frequency variability and a signal due to external forcing. Therefore, it is important to establish the phase and amplitude of the natural variability of the atmospheric circulation.

A major source of the interannual variability in the atmospheric circulation in the North Atlantic region is the North Atlantic Oscillation (NAO). The NAO occurs on a quasi-decadal time scale and is associated with changes in the strength and direction of the surface winds blowing across the North Atlantic to Europe. The NAO index is based on the normalised pressure difference between the Icelandic Low and the Azores High. Hurrell (1995) has calculated this index for all winters from 1864 to 1995, see figure 2. A high NAO index indicates a strong mean zonal flow over the North Atlantic and Europe, and therefore a higher average pressure gradient between Iceland and Portugal. While a low NAO index indicates a lower north-south pressure gradient. Figure 3 shows the difference in the winter average MSLP fields from two 5-year analysis periods. The pattern and magnitude of this difference field is very similar to that of Hurrell (1995), showing the difference in MSLP between years with a high NAO index (greater than 1.0) and years with a low NAO index (less than -1.0) since 1899.

Blocking features in the 500 hPa height field over the North Atlantic, where the basic westerly flow is divided into two branches by the development of a cyclone, also contribute significantly to the low frequency variability. Figure 4 shows the number of blocking days and the number of days with strong zonal flow per winter for the North Atlantic and western Europe calculated for the ECMWF analyses from 1983 to 1992 by Liu and Opsteegh (1995).

5 Verification of the control climate model experiment

We have discussed, in section 4, the problems associated with verifying the climatology of the control experiment. Although the inter-decadal variability of the atmosphere cannot be reproduced in a run of just over five years, we find the climatology of the control experiment to be consistent with the current climate in the sense that the 5-year model climate agrees quite well with a 5-year period from the real climate. We established this by comparing the atmospheric climatology of the control experiment with that from a 5-year period of ECMWF analyses. In particular, we analyse the following parameters: the mean sea level pressure (MSLP), the near surface (10 m) winds and the 500 hPa geopotential height. We will also consider the spatial distribution and frequency of storms over the North Atlantic.

5.1 Mean sea level pressure

We begin with the average winter MSLP field. For the control experiment, this field, figure 5b, appears to compare quite well with the ECMWF analyses for the period 1991-1995, figure 5a, although the average pressure gradient between Iceland and Portugal is slightly weaker in the analyses. This could be explained by arguing that the control experiment is simply a combination of years with a strong average westerly flow. For at least two winters in the control, however, the average gradient is greater than for any of the winters from the ECMWF analyses, including the winter of 1988/89 when the NAO was the highest it has ever been in the last 132 years according to Hurrel (1995). The winter MSLP for the analyses for the 5-year period 1986-90 has an even weaker gradient over the North Atlantic. On this basis, further verification of the control experiment will carried out using the ECMWF analyses for the period 1991-95.

5.2 10 m wind speeds

The climatology of 10 m winds is not normally considered in the analysis of a climate model experiment. However, in this study it is important because the winds are used to simulate waves analysed in section 7.

The average winter 10 m winds from the analyses and the control are comparable, figures 6a and 6b respectively. However, there are some small local differences. Around the British Isles wind speeds are slightly overestimated, while in the central part of the North Atlantic they are underestimated, by as much as 14% in some areas.

There are also some small differences in the variability of the surface wind speed in the control compared with the analyses. In the control the day-to-day (within-month) standard deviation of wind speed, figure 7b, is less than that of the analyses, figure 7a, across most of

the North Atlantic. These differences are small: typically less than 1 m/s but, for example, in the North Sea this represents a difference of about 10%. For a small area off the coast of Northeast Canada and an area along the east coast of Greenland the control overestimates the within-month standard deviation.

The winter extreme wind speeds are estimated by averaging the 10% exceedence values calculated for each winter month. The values for the ECMWF analyses, figure 8a, are greater than those for the control, figure 8b, over most of the North Atlantic and North Sea area. In the central part of the North Atlantic the differences are the greatest, between 1 and 3 m/s. This represents differences of up to 16% in some areas. To the north of the British Isles, however, the extremes in the control are comparable with the analyses.

The differences in the mean, the variability and the extremes of the 10m wind speeds that are seen in figures 6a/b, 7a/b and 8a/b respectively, can be summarised by considering the frequency distributions of wind speeds for six selected areas in the North Atlantic and North Sea, figures 9a-f. The locations of these areas can be seen in figure 1b. For areas 4 and 5, which are the two more southerly areas, the distributions of the wind speeds from the control experiment are slightly more peaked and are shifted to the left. In these areas the average values are slightly lower, the frequency of higher wind speeds is underestimated and the frequency of lower wind speeds is overestimated. For area 1, located to the west of Ireland, and area 6, in the North Sea, the probability distributions of the wind speeds from the control experiment are again slightly more peaked, but they are shifted to the right. In these areas the average values are higher and the frequency of lower wind speeds is underestimated. Also, higher wind speeds are overestimated, although the very extreme values are still underestimated. For the other two areas the distributions compare quite well, except that the frequency of the more extreme winds is again underestimated in the control.

The frequency distributions of wind directions also differ slightly between the control and the analyses, figures 10a-f. For areas 2 and 5, the two most westerly areas, both the control and the analyses give single peak distributions: the dominant direction for area 2 is westerly, while that in area 5 is southwesterly. In both cases the peaks have a higher frequency in the control experiment than the analyses and they are shifted slightly in an anti-clockwise direction. For area 4, west of the Bay of Biscay, the distribution of the analysed wind directions has two peaks, one with a southwesterly direction and the other lower peak with a northeasterly direction. The frequency distribution of the wind directions from the control gives the main peak with a more southerly direction than in the analyses and misses that secondary peak. For areas 1, 3 and 6 there are no systematic differences: in all cases the dominant direction in the control compares well with the analyses, although the peak is too high in area 1.

5.3 500 hPa heights

The time-filtered variability of the winter 500 hPa height field is often used to indicate the position of the storm tracks (Blackmon, 1976). Using a band-pass filter, the variability due to disturbances on the 2.5 to 6 day time scale are preserved. For the climate model control experiment, the position and intensity of the North Atlantic storm track, figure 11b, compare quite well with the analyses, figure 11a. The shape of the storm track is slightly more elongated, extending further both to the west and to the east in the control. The variability over the northeast Atlantic, northwest Europe and east Canada is somewhat overestimated in the control. However, previous climate model experiments at lower resolutions were not able to represent the intensity of the storm track so well. It is details like this that illustrate the advantages of working with data at such a high resolution, even though the period is rather short.

5.4 Storm activity

Since we are dealing with data from a climate model which has a sufficiently high resolution to simulate relatively small scale features, it is interesting to study the storm activity in the North Atlantic area.

We use two methods to evaluate the frequency of storms in the North Atlantic region. In the first method, a storm is identified as a period where the wind speed exceeds a specified threshold for any number of consecutive time steps. In this case the threshold is 15 m/s. In the second method the frequency of cyclones is determined by counting local minima in the MSLP field. The cyclones are categorised according to their core pressure. Note that, in this second method, a cyclone is counted for every time step for which it falls into one of the categories, whereas in the first method, a storm is counted once per lifetime. The first method gives less storms per winter for the control experiment, figure 12b, than for the analyses, figure 12a, except for a small area just to the north of Scotland. On the other hand, the second method gives more storms per winter for the control if we consider only the very deep depressions (< 960 hPa), while the number of depressions with core pressure between 960 and 975 hPa is the same as in the analyses, table 1.

Table 1: Frequency of depressions (per winter) measured by their core pressure in the North Atlantic area for the ECMWF analysis, the control and the 2 x CO_2 time slice experiment.

core pressure of depression, P (hPa)	ECMWF analyses	control experiment	$2xCO_2$ experiment
960 < P < 975	116	117	117
945 < P < 960	39	52	43
P < 945	6	9	10
P < 975	161	178	170

This latter result appears to contradict the previous result. However, the two methods used are quite different. The results of the first method are affected by the pressure gradient around the core of the depressions, while in the second method the duration of each storm is important. We tested to see if either of these factors contributes to the discrepancy, but this appears not to be the case. A further possible explanation for this contradiction is that the two models are different in terms of physics, dynamics, numerics or a combination of the three.

We were able to identify one important difference in the model physics: the Charnock constant used in the ECHAM3 model is 0.032 (DKRZ, 1992), while the value in the ECMWF analysis model is 0.018. There may be other differences in the model physics, but this difference alone is quite probably the cause of the inconsistency between the two methods for estimating the frequency of storms in the North Atlantic area. It may also explain the underestimation of the extreme winds and the underestimation, in some areas, of the average winds.

It was also discovered that there is a difference in the numerical integration schemes used in the ECHAM3 climate model and the ECMWF analysis model. In September 1991 an implicit numerical scheme was introduced in the ECMWF model (Janssen et al., 1992). This scheme treats dynamical and physical processes simultaneously. In the ECHAM3 model, however, different schemes are used to treat the dynamical and physical processes and there is no interaction between them (DKRZ, 1992). This change to the ECMWF model affects the boundary layer scheme near the surface. The main impact is a reduction of the near-surface wind speeds. Based on this information, and given that the average winter MSLP patterns are similar for the analysis (ECMWF) and the control (ECHAM3), see figures 5a/b, we would expect the near-surface wind speeds in the analysis to be lower than those in the control. However, this is not the case. It would seem that the effect of the different model physics, eg a higher Charnock constant, in the ECHAM3 model, outweighs the effect of the different

numerical scheme for extreme winds, in the mid-latitudes at least. For mean wind speeds, however, the effects, more or less, balance out.

Figures 13a and b show the tracks of storms with core pressure less than 950 hPa for the analyses and the control experiment respectively. The locations of the storms in both figures are quite similar.

Using data from the same control time slice experiment, Bengtsson et al. (1995) carried out a similar study of tropical storms. They concluded that the climate model was capable of generating hurricanes with a frequency and distribution comparable to the observed climatology. From the results presented in this report, we can add that storms in the North Atlantic area are also well represented in the climate model.

6 The atmospheric climatology of the 2xCO_2 experiment

The analysis in this section is in the same format as the previous section, but now we compare the climatology of the 2xCO_2 climate model experiment with that of the control, to evaluate the effect of doubling the concentration of atmospheric CO_2 on the atmospheric climatology in the North Atlantic region.

6.1 Mean sea level pressure

The average winter MSLP field for the 2xCO_2 experiment, figure 5c, is comparable with that of the control, figure 5b. The average pressure gradients between Iceland and Portugal are also similar. Figure 5d, shows the anomaly in the average winter MSLP between the control and the 2xCO_2 experiment. In the introduction we looked at the difference field between two different analysis periods, figure 2. In figure 5d there is again a dipole effect, with negative differences of up to 6 hPa over Scandinavia and positive differences of up to 3 hPa over the central North Atlantic. This is associated with a slight extension to the west of the Azores high and an extension to the east of the Icelandic low. The pattern is almost orthogonal to that seen in figure 3, which is associated with an increase in zonal index.

6.2 10 m wind speeds

We now consider the climatology of the 10 m wind speeds. These winds are used to simulate the waves analysed in section 8. The gradient in the anomalies in the average winter MSLP field, figure 6c, is relatively small and almost orthogonal to the mean pressure gradient. Therefore, there is almost no effect on the average winter 10 m wind speeds, figures 6c and 6d. Differences in the day-to-day variability and the extremes of the 10 m wind speeds are similarly small, figures 7c/d and 8c/d respectively.

Referring back to figures 9a-f, the frequency distributions of wind speed for 6 box areas in the North Atlantic and North Sea, we see that the distributions from the 2xCO_2 run (dashed line) are very similar to those from the control (dot-dashed line). In most areas the distributions from the 2xCO_2 run are very slightly shifted to the left, indicating lower average wind speeds and underestimated extreme wind speeds as seen in figure 6c. There are two exceptions to this: areas 4 and 6, where there are no systematic differences between the two distributions.

Looking at the frequency distributions of wind direction for the same box areas, figures 10a-f we can identify, in some areas, a clockwise shift in the distributions of the wind directions in the 2xCO_2 experiment. For example, in area 6, in the North Sea, the dominant wind direction shifts about 30 degrees to a more westerly direction. There is an increase in the frequency of

winds from between southwest and northwest; and a decrease in the frequency of winds from between southeast and southwest. This also occurs in areas 3, 4 and, to some extent, area 1. This result is very interesting because a shift in wind direction to the north of the British Isles would affect the fetch of waves entering the North Sea from a northwesterly direction. There is a higher possibility that waves generated by storms to the east of Greenland will propergate into the North Sea in the $2xCO_2$ simulation because the frequency of northwesterly winds is higher. This situation could lead to an increase in waves heights in the North Sea. However, the results presented in section 8 indicate that such an increase does not occur.

6.3 500 hPa heights

The North Atlantic storm track in the $2xCO_2$ experiment, depicted by the time filtered standard deviation of the winter 500 hPa height field, figure 11c, extends slightly further to the east than in the control and is slightly more intense, figure 11b. The largest increase in the variability at 500 hPa is over Europe, including the North Sea and the Bay of Biscay.

6.4 Storm activity

Relative to the control, figure 12b, the number of storm events distributed over almost the whole of the North Atlantic area decreases slightly in the $2xCO_2$ experiment, by up to 6 events per winter further to the north of the area, figure 12c. This decrease is not so clear in table 1, for the count of storms in terms of depressions, except in the category of cyclones with core pressure between 945 and 960 hPa, where there is a slight decrease.

In general the tracks of cyclones in the $2xCO_2$ experiment, figure 13c, do not differ much from those in the control, figure 13b, although there is a slight decrease in the number of independent storms.

We conclude that, despite the slight increase in the variability of the atmosphere at 500 hPa, the storm activity in the $2xCO_2$ run does not vary significantly from the control. This contrasts the results of Bengtsson et al. (1996), who found a significant decrease in the number of tropical storms (although not in their strength) in the $2xCO_2$ time slice experiment.

7 Verification of waves from the control wave model simulation

In this section we assess the climatology of the total significant wave heights in the control simulation. Verification is done, where possible, using hindcast or analysed wave heights.

7.1 Averages

First we consider the climatology of the average winter wave heights. Figure 14a shows the average winter (DJF) wave height field for the coarse grid and figure 14b shows that for the fine grid. Both plots show a similar pattern for the northeastern Atlantic and North Sea, with an area of maximum wave height of just less than 5.0 m to the northwest of Ireland. In the fine grid the wave heights near the coastlines are slightly reduced as a result of bottom dissipation. In the North Sea average wave heights range from about 1.5 m in the southern tip to 4.5 m to the northeast of Scotland.

In figure 15 the monthly mean wave heights are compared with data from a 40-year hindcast (Lozano et al., 1997a). Six grid points are considered, figures 15a-f: one in the mid-North Sea, one in the northern part of the North Sea, one to the west of Greenland, one to the west of Scotland, one to the west of Ireland and one just off the northwestern coast of Spain. Figure 1b shows the exact locations of these points. To take into account the fact that we are comparing two different periods, a set of 36 5-year running means were calculated for the 40-year hindcast. The average of these means is plotted as a solid line. The two dotted lines represent the minimum and maximum 5-year mean values for each month out of the 36 samples. The mean values for the 5-year control run are shown by the dot-dashed line. In general, the monthly means of the control fall below the average values of the hindcast and, for the greater part, fluctuate around the line representing the minimum values. In the North Atlantic the underestimation of the average monthly wave heights in the control appears to increase inversely with latitude. To the west of Greenland the control values are mostly higher than the minimum values of the 40-year hindcast, while off the northwest coast of Spain the average monthly wave heights of the control are lower for most months of the year. At the stations in the central and northern parts of the North Sea, figures 15a and 15c, the control values compare well with the average values of the hindcast, with relatively high values in February and April. These results indicate that the average wave heights are somewhat underestimated in the control simulation for some parts of the North Atlantic. This agrees with the underestimation, in some areas, of wind speeds, see section 5.2.

Comparisons have also been made with wave height information extracted from the KNMI ship routing charts (Bouws et al., 1996). Area average values are available for box areas 1-5 in the North Atlantic, see figure 1b. Figures 16a-e show the monthly mean values of the box average values. The ship routing data was treated in a similar way to the 40-year hindcast, in

that a set of 5-year running means were calculated for the 23 complete years of data available, resulting in 19 samples. For the most part, the monthly means of the average values of the control fall between the limits of the ship routing data. The exceptions to this are in areas 2 and 4 for some summer months, when the control values are higher than the maximum values from the 23-year ship routing data set; and in areas 1, 3, 4 and 5 in some winter months, when the control values are lower than the minimum values. In area 5 the control values are higher than the average 23-year analysed values throughout the year. These results also indicate, for winter months at least, that the control underestimates the average wave heights in most of the areas considered.

7.2 Standard deviations

Figures 17a and 17b show the day-to-day (within-month) standard deviation of the winter wave heights for the coarse and the fine grid areas respectively. To the southwest of the tip of Greenland there is an local maximum of about 1.8 m. There are another two local maxima just off the ice border along the east coast of Greenland.

7.3 Extremes

The extreme total significant wave heights are estimated by averaging the 10% exceedence values calculated for each winter month. For the control simulation, figure 18a, these extremes are over 7 m in an area to the northwest of Scotland. This area extends slightly further to the west than the area of highest average wave heights seen in figure 17a, as can be expected from the higher variability of the wave heights further to the west. Extreme wave heights are between 1.0 m and 6.0 m in the North Sea.

Again, we can refer to the 40-year hindcast to verify the 10% exceedence values of the control. Figure 19 compares the averaged monthly 10% exceedence values for 6 selected grid points. The location of these points is the same as in figure 15. As with the average monthly values, it is striking that the monthly extreme values of the control are mostly lower than the average values from the 40-year hindcast. And at all the six grid points there are months where the control values fall below the minimum 5-year values of the hindcast.

From the KNMI ship routing charts, the monthly means of the box maximum wave heights are also used to compare with those from the control for box areas 1-5. In all areas the average values for the control are less than those for the ship routing data, figure 20. In areas 1-4 the average values for the control are also less than or equal to the minimum values for each month of the ship routing data set.

For both the grid point analysis and the box area analysis there is a strong suggestion that

wave heights are underestimated in the control. This is in agreement with the underestimation of extreme winds in the control time slice experiment, see section 5.2.

7.4 Frequency distributions

The results that have been presented so far in this section can be summarised by looking at the frequency distributions of wave heights for box areas 1-5, figure 1b. In figures 21a-e the frequency distributions calculated from the 40-year hindcast are shown as a solid line. The probabilities are calculated by taking the average of the 5-year running mean values for each frequency bin. In this case a bin is 0.5 m. The maximum and minimum 5-year mean values for each bin are shown by the dotted lines. Strictly speaking, these two lines are not correct, in the sense that the area under these distributions is not equal to one. But they are useful in that they indicate, for each frequency bin, the range of the 5-year mean values calculated from the 40-year hindcast. The frequency distribution of the wave heights from the five winters of the control simulation are given as dot-dashed lines. The same characteristics can been seen in all the box areas. Namely that the control distributions are more sharply peaked than the hindcast distributions. In all areas the means and the extremes are underestimated in the control. Also, in areas 4 and 5 the distribution of the control is shifted to the left so that the frequency of lower wave heights is higher compared to the hindcast. Also the frequency of wave heights greater than about 3.5 m is notably underestimated, even compared to the minimum values of the 36 samples from the 40-year hindcast. This confirms the tendency of the control to underestimate the means and extremes of the wave heights for the areas studied.

7.5 20-year return values

Extreme value analysis has been carried out by Gomez et al. (1997) on the total significant wave heights in the fine grid. For this analysis 30 independent peaks were selected for each grid point from the whole 5-year time series of wave heights. These values were then fitted to a statistical distribution which was extrapolated to give extreme wave heights with various return periods. The extreme waves presented in this report are the 20-year return wave heights estimated by fitting the Gumbel distribution to the data. The estimated wave heights with a return period of 20 years for the control simulation, figure 22a, are greater than 12 m for most of the central North Atlantic area. In the North Sea, values range from 4 m to 11 m. These values are somewhat low compared to those calculated by Korevaar (1990). The 10-year return wave heights that he calculated for the North Sea, based on visual observations, range from 6 to 16 m. This underestimation agrees with the other results that we have seen in section 7.

8 The wave climatology of the 2xCO_2 simulation

In this section we assess the sensitivity of wave heights to the small differences in the wind climatology given in the 2xCO_2 time slice experiment.

8.1 Averages

The total significant wave heights of the 2xCO_2 simulation are compared with those from the control simulation. First we look at the average climatology. Figures 14c and 14d show the average winter total significant wave height differences (2 x CO_2 - control) for the coarse and the fine grid areas respectively. The general pattern for the North Atlantic and North Sea shows two areas of positive differences, one off the eastern coast of North America, and one to the northwest of the European continent, separated by negative differences in most of the rest of the area. The area of positive differences in the North sea is more clearly seen in the plot of the fine grid area. In this plot there is a maximum increase of about 16 cm off the coast of the Netherlands, where the mean for the control was between 1.6 and 2.0 m: an increase of only 1%. The pattern in Figure 14c strongly resembles that in Figure 6d which shows the differences in the winter average 10 m wind speeds between the 2xCO_2 time slice experiment and the control. However, the relative magnitude of the positive increases in the wave heights is smaller than that in the wind speeds. In other words, the difference pattern of the average wave climatologies is simply a smoothed version of the difference pattern of the average wind climatology.

For the six grid points analysed, it can be seen that the monthly mean wave heights do not vary a great deal between the control and the 2xCO_2 run. In figure 15, the dashed lines of the 2xCO_2 run follow the dot-dashed line of the control quite closely. In cases where there are somewhat larger differences, for example in March for grid points 4 and 12, which both lie in the North Sea, the differences are less than that of the range of the running means calculated for the 40-year hindcast, indicated by the dotted lines. The differences are therefore probably not significant.

Similarly, for the 5 box areas, the differences between the monthly mean wave heights in the 2xCO_2 simulation and the control are relatively small, figure 16.

8.2 Standard deviations

The difference field of the within-month standard deviations for the coarse grid area, figure 17c, is rather noisy. There are areas of positive differences: one stretching across the central North Atlantic from the west coast of France to the east coast of the North America; and one to the north of the British Isles, which stretches up to the ice boundary, north of Iceland. This

indicates a slight increase in the variability of wave heights in these areas. The same field for the fine grid area, figure 17d, also shows these areas of positive differences in slightly more detail.

8.3 Extremes

The differences in the extreme wave heights, as given by the monthly averaged 10% exceedence values, figures 18c and 18d, give a pattern very similar to that of the differences in the average wave heights, as seen in figures 14c and 14d. To the west of North America the increase in the extreme wave heights from $2xCO_2$ simulation are up to 0.4 m, while in the North Sea and the Bay of Biscay, differences are as high as 0.55 m. The difference pattern is similar to the corresponding pattern for the 10 m wind speeds, figure 8d. Once again the magnitude of the positive differences is smaller than for the wind speeds.

Looking at the 6 selected grid points the monthly mean values of extreme waves for the $2xCO_2$ simulation (dashed line) do not systematically vary from those of the control (dot-dashed line), figure 19. This is also true for the 5 box areas analysed, figure 20.

8.4 Frequency distributions

Figures 22a-e, show that the distributions of wave heights in the 2 x CO_2 are also very similar to those in the control for box areas 1-5. In all areas the frequency distributions are shifted slightly to lower wave heights in the 2 x CO_2 run. This means that the mean and extreme values are lower, while the probability of lower wave heights is higher in the $2xCO_2$ simulation. However, in each case, the magnitude of this shift is very small, less than the range of the 5-year running values calculated for the 36 samples from the 40-year hindcast. This reflects the results seen in the previous figures, and we conclude that the waves from the $2xCO_2$ simulation are not significantly different from those of the control.

8.5 20-year return values

The differences in the estimated wave heights with a return period of 20 years are shown in figure 22b. These differences are as high as 4 m to the south of Iceland and 3 m in the North Sea. These values represent percentage differences of about 40% relative to the control values. This appears to be a rather strong signal. However, the magnitude of the errors is comparable to that of the differences in the 20-year return values between the two simulations. Figures 23a and 23b show the errors (+/- m) for the control and the $2xCO_2$ simulation respectively based on the 95% confidence intervals for each point. The differences seen in figure 22b are therefore not statistically significant. This is consistent with the results we have obtained earlier in this section.

9 Summary

9.1 Atmospheric climatology - control

In general, the atmospheric climate of the control experiment in the North Atlantic area compares well with that of the ECMWF analyses for the period 1991-1995. There are, however, some differences. The control run has a slightly stronger average MSLP gradient across the North Atlantic. There is a tendency for the zonal index in some individual years of the control to be rather stronger than in any individual year from the ECMWF analyses. Also, the storm track is slightly elongated in the control. Given these differences, we would expect the control to overestimate the wind speeds. However, the means, extremes and variability of the 10 m wind speeds are all underestimated to some extent in the control run. This is probably caused by differences in the model physics used in the ECHAM3 AGCM and the ECMWF analysis model.

9.2 Atmospheric climatology - 2xCO_2 scenario

There are some regional differences between the control and the 2xCO_2 experiments. But these are all relatively small compared to the differences between the analyses and the control. They are less than the natural variability and can therefore probably not be attributed to the effects of external forcing. However, it is still interesting to consider the difference patterns between the control and the 2xCO_2 scenario.

The average MSLP gradient between Portugal and Iceland in the 2xCO_2 experiment is very similar to that of the control. However, the Icelandic low extends further to the east and the Azores high extends further to the west. This is seen in the anomaly pattern quite clearly, figure 5d. The net effect, however, on the average winter wind speed is minimal. The area plots of the extreme 10 m wind speeds and the within-month standard deviations are also, on the whole, unchanged. This is reflected in the probability distributions of wind speed for selected grid points.

The distributions of wind direction in the 2xCO_2 experiment differ, in some areas, from those in the control. In four of the areas considered, all of which lie in the northeasterly part of the Atlantic or in the North Sea, there is an increase in the frequency of winds from westerly and northwesterly directions and a decrease in winds from the south and southeast. In the North Sea area, the area to the west of Spain and the area to the north of Scotland the dominant direction veers by about 30 degrees.

The North Atlantic storm track extends slightly further to the east and the southeast in the 2xCO_2 experiment than in the control. This is associated with an increase in the spatial

pattern of the frequency of storm events, which shows an increase in the Bay of Biscay and the North Sea. There are, however, decreases in this pattern in the rest of the North Atlantic. The count of deep cyclones over the whole area shows a slight decrease in the $2xCO_2$ run.

9.3 Wave climatology - control

The monthly mean and the monthly extreme wave heights for selected grid points in the control simulation of the wave climate are mostly lower than average calculated from the 40-year hindcast, but never significantly lower than the minimum values. The monthly means for winter months and the monthly extremes are also underestimated compared with the wave heights extracted from the 23-years of ship routing data. This underestimation is not unexpected, since we have already seen that the wind speeds are also underestimated compared with the ECMWF analysis. The probability distributions of wave height also show that both the mean and extreme values are underestimated in the control with respect to the 40-year hindcast. Furthermore, the 20-year return wave heights are also underestimated compared to a previous study (Korevaar, 1990).

9.4 Wave climatology - $2xCO_2$ scenario

The total significant wave height in the $2xCO_2$ simulation decreases in the Norwegian sea and the central part of the Atlantic, while there are some increases of up to 1% in the North Sea and in the western part of the Atlantic. The extreme values of the wave height also increase slightly in the North Sea and there are higher values off the east coast of Canada. These slight increases in the averages and extremes of the wave heights are associated with small increases in the average wind speeds and the extreme wind speeds in the $2xCO_2$ run in the same areas. There is no evidence that the veering of the wind seen in the $2xCO_2$ run has a significant impact on wave heights in the North Sea.

For the grid points studied, the average monthly values and the monthly extreme values of the $2xCO_2$ wave simulation do not vary systematically from the control. However, there are small decreases in the values for the $2xCO_2$ simulation for the winter months at the grid points considered in the northeast Atlantic, and small increases in the southern part of the North Sea. This is in agreement with the maps of average and extreme wave heights. Also the differences between the control and the 40-year hindcast are larger than the differences between the $2xCO_2$ simulation and the control.

The probability distributions of wave heights for the two simulations reflect the small differences seen in the plots for the North Atlantic area. The distributions from the $2xCO_2$ simulation tend to be shifted to lower values of wave height. These differences are very small compared to the differences between the control and the ECMWF analyses. However, this is

not a very good measure for the significance of the difference between the two wave simulations since we suspect that the forcing winds are underestimated.

The extreme wave analysis carried out on the wave heights from the two simulations indicates relatively large anomalies in the 20-year return wave heights for the $2xCO_2$ simulation. To the south of Iceland there is an area of relatively large increases, while further to the south there are decreases in these values. This partly represents a shift in the position of maximum values in the $2xCO_2$ simulation compared to the control. However the errors, estimated by the 95% confidence interval are of the same magnitude as the anomalies. Therefore, these differences are not statistically significant.

10 Conclusions

The atmospheric circulation over the North Atlantic region is strongly influenced by low-frequency natural variability. This means that the climate model time slices of just over five years, which we have analysed, are not sufficiently long enough to make conclusive statements about changes in the climate due to increased atmospheric concentrations of CO_2. Therefore care must be taken when interpreting the analysis of climate model data.

The atmospheric climate of the control climate model experiment in the North Atlantic area seems to be consistent with the current climate. In particular, the North Atlantic storm track and the frequency of deep depressions are well represented in the climate model. This has not been achieved previously with lower resolution models.

There is some evidence, however, that the extreme wind speeds and, in some areas the mean wind speeds are underestimated in the climate model. The climatology of the wave heights in the control simulation is therefore also somewhat underestimated compared to hindcast data and analysed data. This should be confirmed in a future study by making comparisons with satellite data.

Despite the underestimation of the winds and waves, it is still useful to consider the differences in the wind and wave climatologies between the control and the $2xCO_2$ scenario. This gives us an estimate of the relative effect of increased atmospheric CO_2 concentrations.

The atmospheric climate of the $2xCO_2$ climate model experiment in the North Atlantic area differs locally from the control in some aspects. These differences are reflected in the climatology of the $2xCO_2$ wave simulation, although the magnitude and pattern of the differences are somewhat smoothed. We cannot conclude that these differences are induced by external forces, considering the large natural variability of the atmosphere.

The extreme wave analysis shows a rather stronger signal in the $2xCO_2$ simulation. The difference pattern ($2xCO_2$ - control) shows an area of positive differences to the northwest of the British Isles, and an area of negative differences to the south west of the British Isles. However, the errors in the estimated extreme values have the same magnitude as the differences.

We conclude that, with respect to storms and waves in the North Atlantic area, the $2xCO_2$ simulation is not significantly different from that of the control. The anomalies in the wave climatology are not larger than expected given the anomalies in the wind climatology.

Acknowledgements

The authors are grateful to Prof. L. Bengtsson for giving his permission to access the ECHAM3/T106 time slice experiments; to the Joint Coordinating Committee for the European Climate Computer Network for supplying computer resources, to Joachim Biercamp for his assistance in managing these resources; to ECMWF for supplying computer resources and making the analysis data available; to John Greenaway for his assistance in ECMWF computer matters; to Graeme Walker and Pauline Gabbitass for transferring data produced at ECMWF to cartridges; to Marek Stawarz for making data available from the 40-year hindcast; and to Ignacio Lozano and Marta Gomez Lahoz for carrying out the extreme value analysis on the two climate wave simulations. Thanks also to Robert Mureau for his useful comments on this report.

This work is part of the EU sponsored WASA project (grant no. EV5V-CT94-0506).

Bibliography

Alexandersson, H., K. Iden and T. Schmith, 1997: Using the triangle method to reconstruct a proxy wind climate during the 20th century in the North Atlantic. To appear in special issue of *Global Ocean Atmos. Sys.* in 1997.

Bacon, S., and D. J. T. Carter, 1991: Wave climate changes in the North Atlantic and North Sea. *Int. J. Climatology*, **11**, 545-558.

Beersma, J.J., 1994: Storm activity over the North Sea and the Netherlands in two climate models compared with observations. KNMI Scientific report WR 94-02, 43pp., KNMI, De Bilt, The Netherlands.

Beersma, J., K. Rider, G. J. Komen, E. Kaas and V. Kharin, 1996: An analysis of extra-tropical storms in the North Atlantic region as simulated in a control and a $2xCO_2$ time-slice experiment with a high resolution atmospheric model. Submitted to *Tellus*.

Bengtsson, L., M. Botzet and M. Esch, 1995: Hurricane-type vortices in a general circulation model, Part I. *Tellus*, **47A**, 175-196.

Bengtsson, L., M. Botzet and M. Esch, 1996: Will greenhouse gas-induced warming over the next 50 years lead to higher frequency and greater intensity of hurricanes? *Tellus*, **48A**, 57-73.

Bijl, W., R. Flather, M. Reistad, J.G. de Ronde, T. Schmith and H. von Storch., 1997: Changing storminess? an analysis of long-term sea-level, wave height and wind data sets. To appear in special issue of *Global Ocean Atmos. Sys.* in 1997.

Blackmon, M.L., 1976: A climatological spectral study of the 500mb geopotential height of the Northern Hemisphere. *J. Atmos. Sci.*, **33**, 1607-1623.

Bouws, E., D. Jannink and G.J. Komen, 1996: On the increasing wave height in the North Atlantic Ocean. To appear in *Bull. Amer. Meteor. Soc.*.

Collier, C.G., J. Dixon, M.S.J. Harrison, J.C.R. Hunt, J.F.B. Mitchell and D.S. Richardson, 1994: Extreme surface winds in mid-latitude storms: forecasting and changes in climatology. *J. of Wind Eng.* Ind. Aerodyn., **52**, 1-27.

Cubasch, U., K. Hasselmann, H. Hoeck, E. Maier-Reimer, U. Mikolajewicz, B.D. Santer and R. Sausen, 1992: Time-dependent greenhouse warming computations with a coupled ocean-atmosphere model. *Clim. Dyn.*, **8**, 55-69.

DKRZ, 1992: The ECHAM 3 atmospheric general circulation model. DKRZ Technical Report No.6, 184 pp., DKRZ, Hamburg, Germany.

Dronia, 1991: On the accumulation of excessive low pressure systems over the North Atlantic during the winter seasons (November to March) 1988/89 to 1990/91. *Die Witterung im*, **39**, 27.

Flather, R. and J. Smith, 1997: Article to appear in special issue of *Global Ocean Atmos. Sys.* in 1997.

Gomez Lahoz, M. and I. Lozano, 1997: Article to appear in special issue of *Global Ocean Atmos. Sys.* in 1997.

Hall, N.M.J., B.J. Hoskins, P.J. Valdes, and C.A. Senior, 1994: Storm tracks in a high-resolution GCM with doubled carbon dioxide. *Q. J. R. Meteorol. Soc.*, **120**, 1209-1230.

Held, I.M., 1993: Large-scale dynamics and global warming. *Bull. Amer. Meteor. Soc.*, **74**, 228-241.

Hogben, N., 1994: Increases in wave heights over the North Atlantic: a review of the evidence and some implications for the naval architect. *Roy. Inst. Naval Arch.*, 93-101.

Hurrel, J.W., 1995: Decadal trends in the North Atlantic Oscillation: Regional temperatures and precipitation. *Science*, **269**, 676-679.

Janssen, P.A.E.M., A.C.M. Beljaars, A. Simmons and P. Viterbo, 1992: The Determination of the Surface Stress in an Atmospheric Model. *Mon. Wea. Rev.*, **120**, 2977-2985.

Kattenberg, A., F. Giorgi, H. Grassl, G.A. Meehl, J.F.B. Mitchell, R.J. Stouffer, T. Tokioka, A.J. Weaver and T.M.L. Wigley, 1996: Climate Models - Projections of Future Climate Change. *Climate Change 1995, The Science of Climate Change*, J.T. Houghton, L.G. Meira Filho, B.A. Callander, N. Harris, A. Kattenberg and K. Maskell, Eds., Cambridge University Press, Cambridge, UK, 572 pp.

Kaas, E., T-S. Li, and T. Schmith, 1996: Statistical hindcast of wind climatology in the North Atlantic and Northwestern European region. Accepted for publication in *Clim. Res.*.

Komen, G.J, L. Cavaleri, M. Donelan, K. Hasselmann, S. Hasselmann, P.A.E.M. Janssen, 1994: Dynamics and modelling of ocean waves. Cambridge University Press, Cambridge, UK, 532 pp.

Korevaar, C.G., 1990: North Sea climate based on observations from ships and lightvessels. Kluwer Academic Publishers, Dordrecht, 137pp.

Lambert, S.J., 1992: Cyclones, intraseasonal variability and the greenhouse effect. 2nd Int. Conf. on Modelling of Global Climate Change and Variability, Hamburg 7-11 September, 1992.

Lozano, I., M. Gomez Lahoz, J.C Carretero, M. Reistad, M. Stawarz, H. Günther and W. Rosenthal, 1997a: The WASA wave hindcast. To appear in special issue of *Global Ocean Atmos. Sys.* in 1997.

Lozano, I., M. Gomez Lahoz, O. Serrano, M. Reistad, M. Stawarz, H. Günther and W. Rosenthal, 1997b: The WASA wave hindcast statistics. To appear in special issue of *Global Ocean Atmos. Sys.* in 1997.

Liu, Q. and T. Opsteegh, 1995: Interannual and Decadal Variations of the Blocking-activity in a Quasi-geostrophic Model, *Tellus,* **47A**, 941-954.

Mietus, M., 1997: Article to appear in special issue of *Global Ocean Atmos. Sys.* in 1997.

Nicholls, N., G.V. Gruza, J. Jouzel, T.R. Karl, L.A. Ogallo and D.E. Parker, 1996: Observed Climate Variability and Change. *Climate Change 1995, The Science of Climate Change*, J.T. Houghton, L.G. Meira Filho, B.A. Callander, N. Harris, A. Kattenberg and K. Maskell, Eds., Cambridge University Press, Cambridge, UK, 572 pp.

Rider, K., 1996: A description of the WASA data sets. KNMI Scientific report, KNMI, De Bilt, The Netherlands.

Schinke, H., 1993: On the occurrence of deep cyclones over Europe and the North Atlantic in the period 1930-1991. *Beitr. Phys. Atmosph.*, **66**, 223-237.

Schmidt, H. and H. von Storch, 1993: German Bight storms analysed. *Nature*, **365**, 791.

Schmith, T., and E. Kaas, 1997: Storm climate at 15 stations in the North Sea during the 20th century: trends, variability and relationship to large scale mean flow. To appear in special issue of *Global Ocean Atmos. Sys.* in 1997.

Stein, O. and A. Hense, 1994: A reconstructed time series of the number of extreme low pressure events since 1880. *Meteorol. Zeitschrift*, **N.F.3**, 43-46.

van Hooff, R.W., 1993: Trends in the wave climate of the Atlantic and North Sea and implication. *Underwater Tech.*, **19**(4), 20-23.

von Storch, H., J. Guddal, K.A. Iden, T. Jonsson, J. Perlwitz, M. Reistad, J. de Ronde, H. Schmidt and E. Zorita, 1993: Changing statistics of storms in the North Atlantic? MPI Report No. 116, 19 pp, MPI, Hamburg, Germany.

von Storch, H. et al., 1997: Article to appear in special issue of *Global Ocean Atmos. Sys.* in 1997.

WASA group, 1995: The WASA project: changing storm and wave climate in the northeast Atlantic and adjacent seas? Fourth international workshop on wave hindcasting and forecasting, Banff, Canada, October 16-20, 1995.

Figure captions

Figure 1: Locations of a) grid points and box areas used for comparison of data and b) the wave model grid areas (coarse: 20N to 80N, 78W to 48E; fine: 38N to 77N, 30W to 45E).

Figure 2: Winter (December to March) index of the North Atlantic Oscillation (NAO) based on the difference of normalised pressures between Lisbon, Portugal, and Stykkisholmur, Iceland, from 1864 to 1996 (Hurrel, 1995).

Figure 3: Difference in the average winter (December to February) mean sea level pressure over the North Atlantic area between two 5-year periods of ECMWF analyses (1991-1995 minus 1986-1990).

Figure 4: Number of blocking and strong zonal flow days per winter (December to February) over the North Atlantic and western Europe in the ECMWF analyses, from 1983 to 1992 (Liu & Opsteegh, 1995).

Figure 5: Average winter (December to February) mean sea level pressure over the North Atlantic area for a) the ECMWF analyses (1991 to 1995), b) the control (6 winters) and c) the $2xCO_2$ scenario (6 winters).

Figure 6: Average winter (December to February) 10 m wind speeds over the North Atlantic area for a) the ECMWF analyses (1991 to 1995), b) the control (6 winters) and c) the $2xCO_2$ scenario (6 winters).

Figure 7: Within-month standard deviation of winter (December to February) 10 m wind speeds over the North Atlantic area for a) the ECMWF analyses (1991 to 1995), b) the control (6 winters) and c) the $2xCO_2$ scenario (6 winters).

Figure 8: 10% exceedence values of winter (December to February) 10 m wind speeds over the North Atlantic area for a) the ECMWF analyses (1991 to 1995), b) the control (6 winters) and c) the $2xCO_2$ scenario (6 winters).

Figure 9: Frequency distributions (%) of winter (December to February) 10 m wind speeds for 6 box areas in the North Atlantic and North Sea, see figure 1b for locations. Solid line: ECMWF analyses (1991 to 1995); dot-dashed line: the control (5 winters); dashed line: the $2xCO_2$ scenario (5 winters).

Figure 10: Frequency distributions (%) of winter (December to February) 10 m wind directions for 6 box areas in the North Atlantic and North Sea, see figure 1b for locations. Solid line: ECMWF analyses (1991 to 1995); dot-dashed line: the control (5 winters); dashed line, the $2xCO_2$ scenario (5 winters)

Figure 11: Standard deviation of the band-pass (2.5-6 days) filtered winter (December to February) 500 hPa heights over the North Atlantic area for a) the ECMWF analyses (1991 to 1995), b) the control (6 winters) and c) the $2xCO_2$ scenario (6 winters).

Figure 12: Number of storm events per winter (December to February) over the North Atlantic area for a) the ECMWF analyses (1991 to 1995), b) the control (6 winters) and c) the $2xCO_2$ scenario (6 winters). See text for further details.

Figure 13: Tracks of cyclones with core pressure < 950 hPa in the North Atlantic area for a) the ECMWF analyses (1991 to 1995) (30 independent storms), b) the control (5 winters) (41 independent storms) and c) the $2xCO_2$ scenario (5 winters) (36 independent storms).

Figure 14: Average winter (December to February) total significant wave heights in the North Atlantic and North Sea for a) the control, coarse grid (5 winters), b) the control, fine grid (5 winters), c) the $2xCO_2$ scenario minus the control, coarse grid (5 winters) and d) the $2xCO_2$ scenario minus the control, fine grid (5 winters).

Figure 15: Monthly average values of total significant wave heights for 6 selected grid points in the North Atlantic and North Sea, see figure 1b for locations. Solid line: averages of the 5-year running means from the 40-year hindcast; dotted lines: maximum and minimum values of the 5-year running means from the 40-year hindcast; dot-dashed line: the control (5 years); dashed line: the $2xCO_2$ scenario (5 years).

Figure 16: Monthly average values of the area means for 5 box areas in the North Atlantic, see figure 1b for locations. Solid line: averages of the 5-year running means from the 23-year ship-routing data set; dotted lines: maximum and minimum values of the 5-year running means from the 23-year ship-routing data set; dot-dashed line: the control (5 years); dashed line: the $2xCO_2$ scenario (5 years).

Figure 17: Within-month standard deviation of winter (December to February) total significant wave heights in the North Atlantic and North Sea for a) the control, coarse grid (5 winters), b) the control, fine grid (5 winters), c) the $2xCO_2$ scenario minus the control, coarse grid (5 winters) and d) the $2xCO_2$ scenario minus the control, fine grid (5 winters).

Figure 18: 10% exceedence values of winter (December to February) total significant wave heights in the North Atlantic and North Sea for a) the control, coarse grid (5 winters), b) the control, fine grid (5 winters), c) the $2xCO_2$ scenario minus the control, coarse grid (5 winters) and d) the $2xCO_2$ scenario minus the control, fine grid (5 winters).

Figure 19: Monthly 10% exceedence values of total significant wave heights for 6 selected grid points in the North Atlantic and North Sea, see figure 1b for locations. Solid line: averages of the 5-year running 10% exceedence values from the 40-year hindcast; dotted lines: maximum and minimum values of the 5-year running 10% exceedence values from the 40-year hindcast; dot-dashed line: the control (5 years); dashed line: the $2xCO_2$ scenario (5 years).

Figure 20: Monthly average values of the area maxima for 5 box areas in the North Atlantic and North Sea, see figure 1b for locations. Solid line: averages of the 5-year running maximums from the 23-year ship-routing data set; dotted lines: maximum and minimum values of the 5-year running maximums from the 23-year ship-routing data set; dot-dashed line, the control (5 years); dashed line: the $2xCO_2$ scenario (5 years).

Figure 21: Frequency distributions (%) of winter (December to February) total significant wave heights in 5 box areas in the North Atlantic and North Sea, see figure 1b for locations. Solid line: averages of the 5-year running mean frequencies from the 40-year hindcast; dotted lines: maximum and minimum values of the 5-year running mean frequencies from the 40-year hindcast; dot-dashed line: the control (5 winters); dashed line: the $2xCO_2$ scenario (5 winters).

Figure 22: Estimated 20-year return values of total significant wave height for the North Atlantic and the North Sea (calculated by fitting the Gumbel distribution) for a) the control, fine grid (5 years) and b) the $2xCO_2$ scenario minus the control, fine grid (5 years).

Figure 23: Errors in the estimated 20-year return values of total significant wave height for the North Atlantic and the North Sea (calculated by fitting the Gumbel distribution) for a) the control, fine grid (5 years) and b) the $2xCO_2$ scenario, fine grid (5 years).

Figure 1a

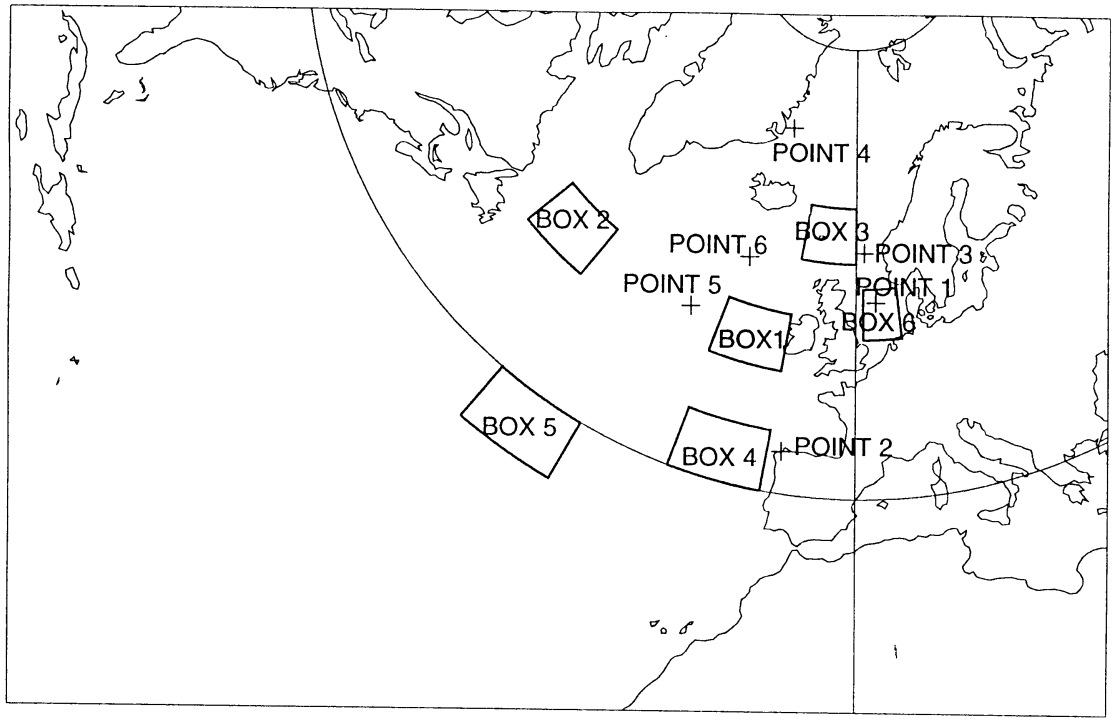

Figure 1b

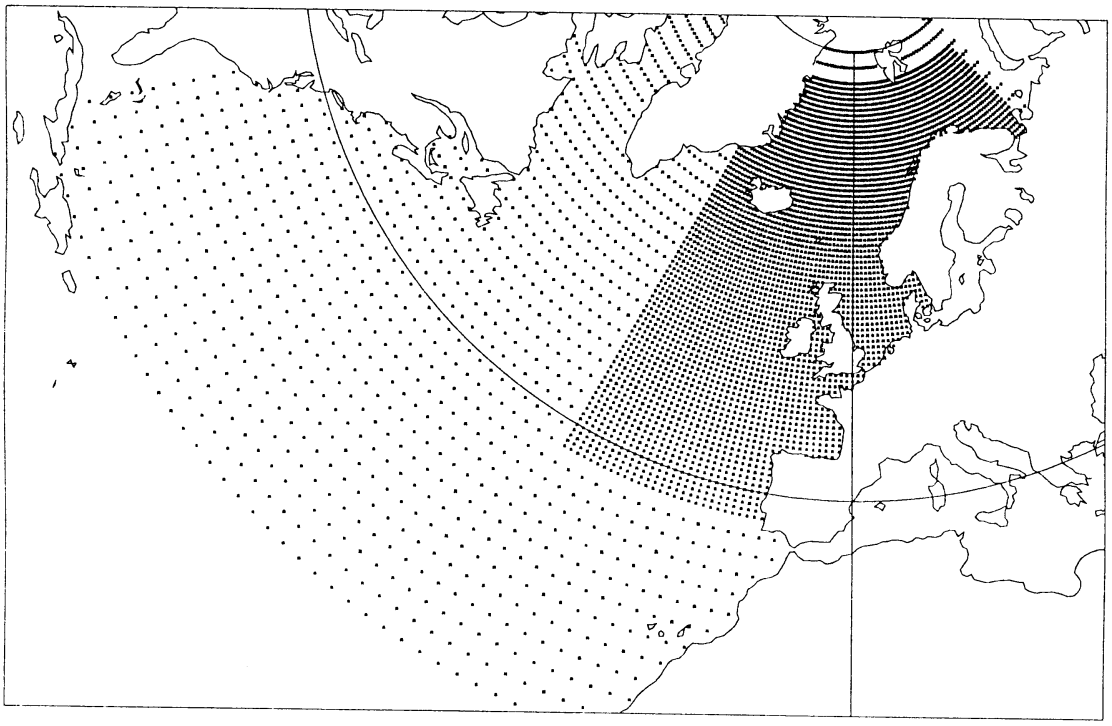

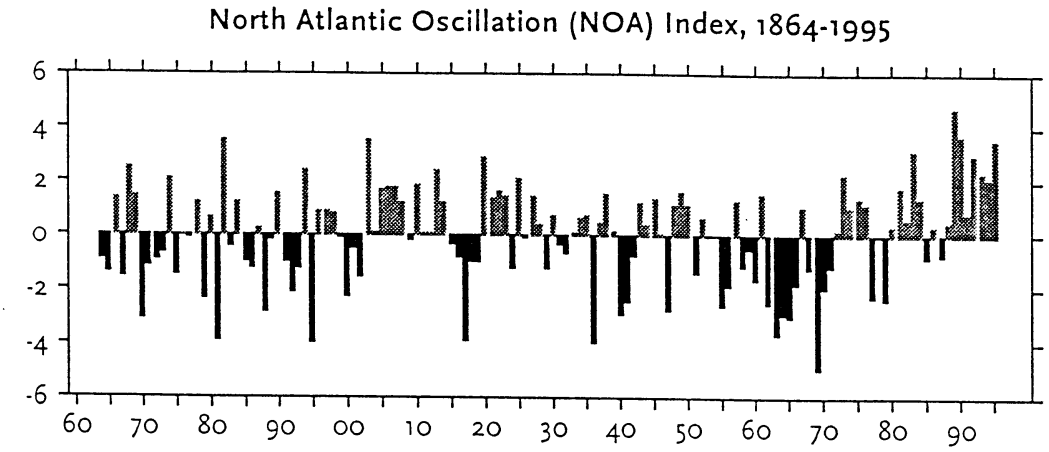

Figure 2: Winter (December to March) index of the North Atlantic Oscillation (NAO) based on the difference of normalised pressures between Lisbon, Portugal, and Stykkisholmur, Iceland, from 1864 to 1996 (Hurrel, 1995).

Figure 3

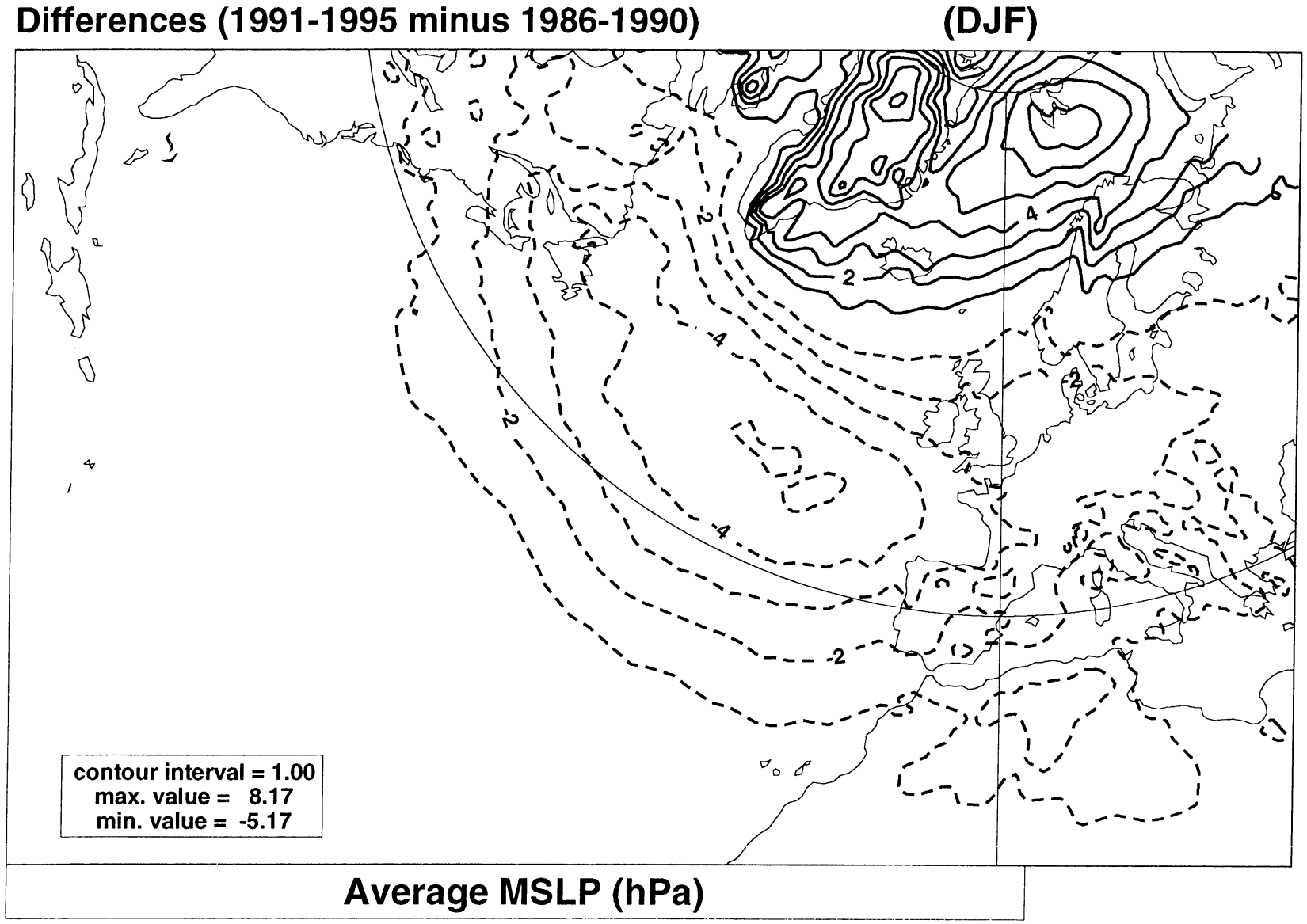
Differences (1991-1995 minus 1986-1990)
(DJF)
4
2
-2
-4
-2
-4
-2
contour interval = 1.00
max. value = 8.17
min. value = -5.17
Average MSLP (hPa)

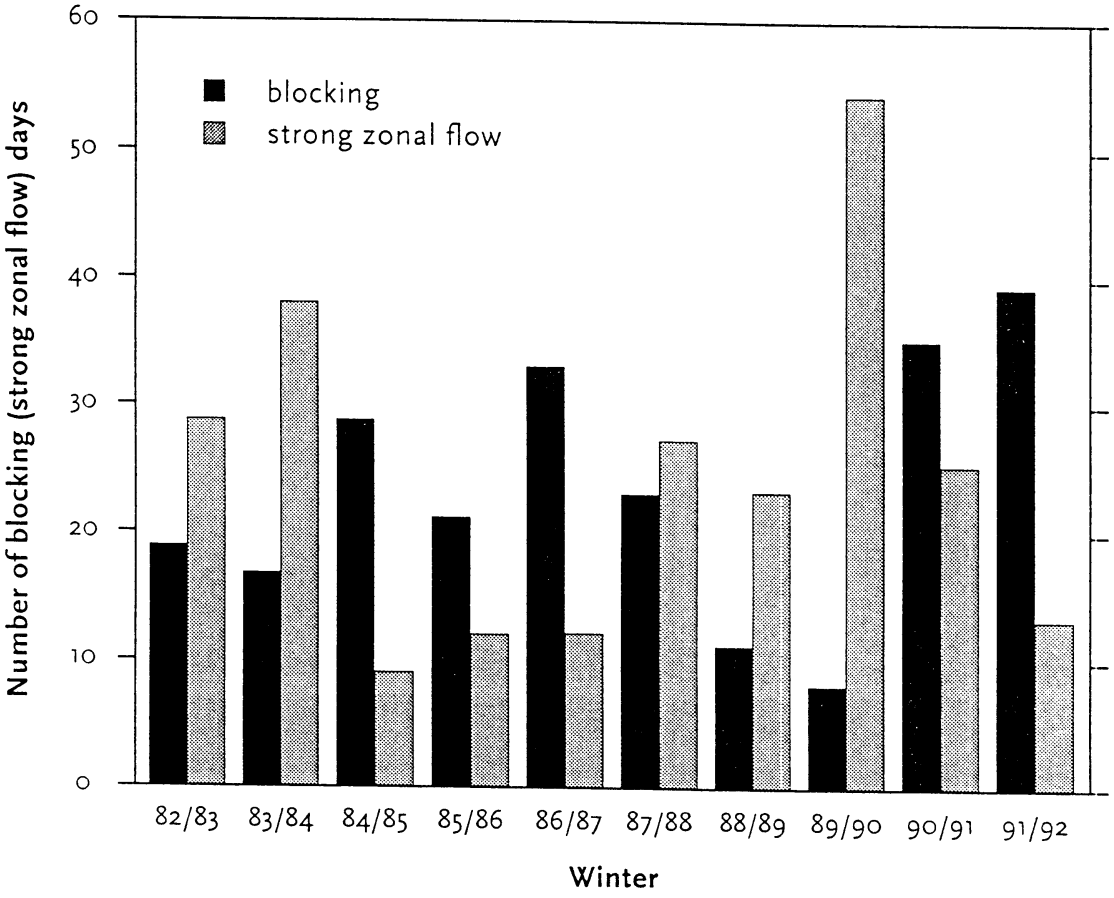

Figure 4: Number of blocking and strong zonal flow days per winter (December to February) over the North Atlantic and western Europe in the ECMWF analyses, from 1983 to 1992 (Liu & Opsteegh, 1995).

Figure 5.a

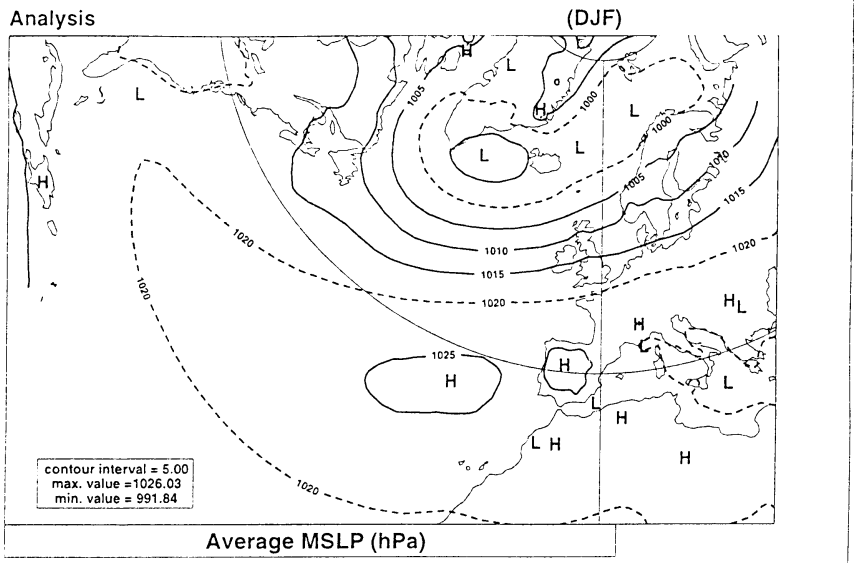

Figure 5.b

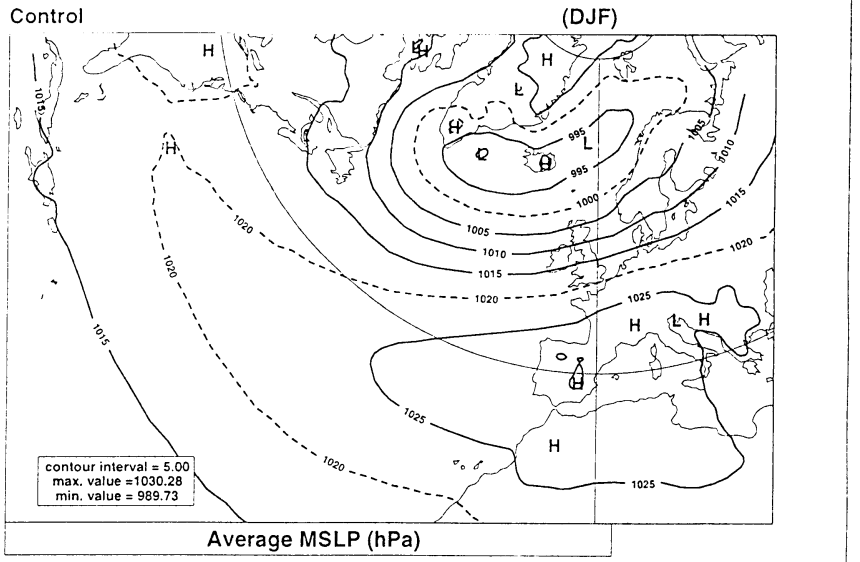

Figure 5.c

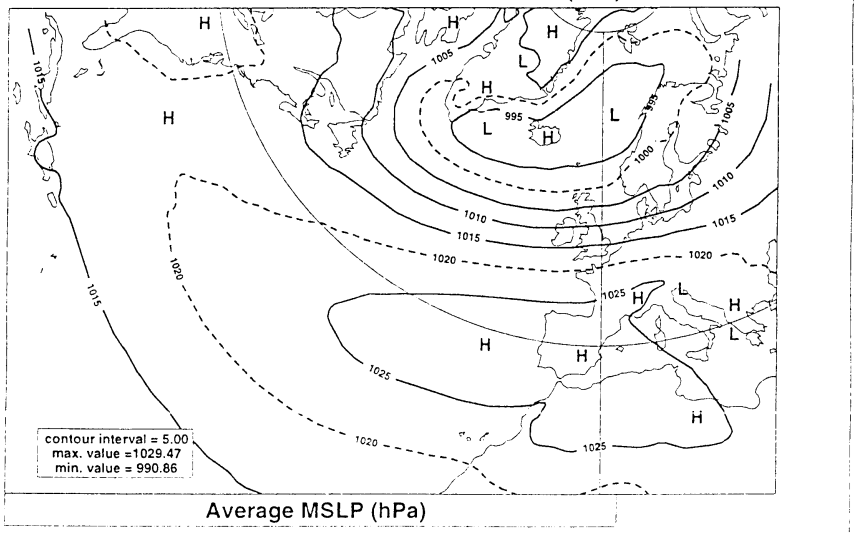

Figure 5.d

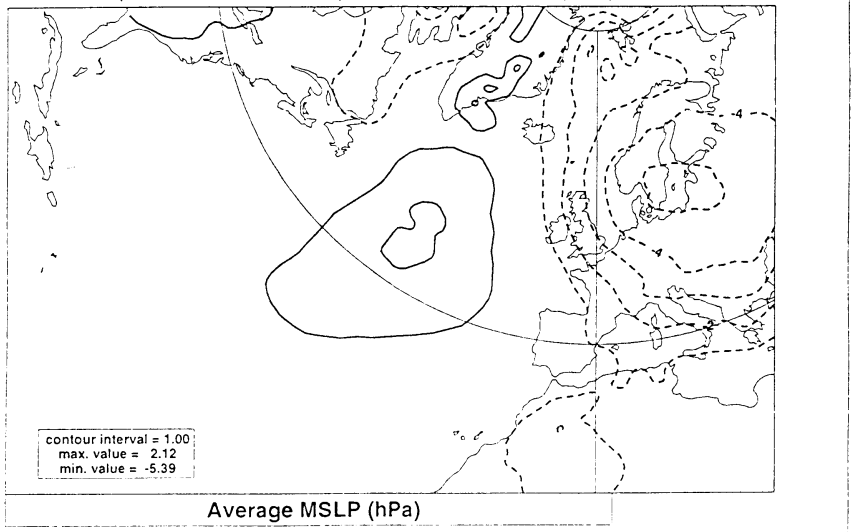

Figure 6.a

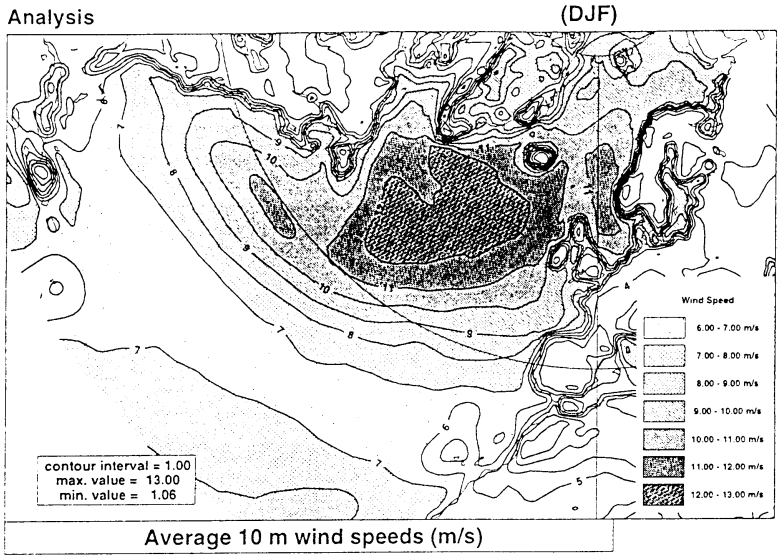

Figure 6.b

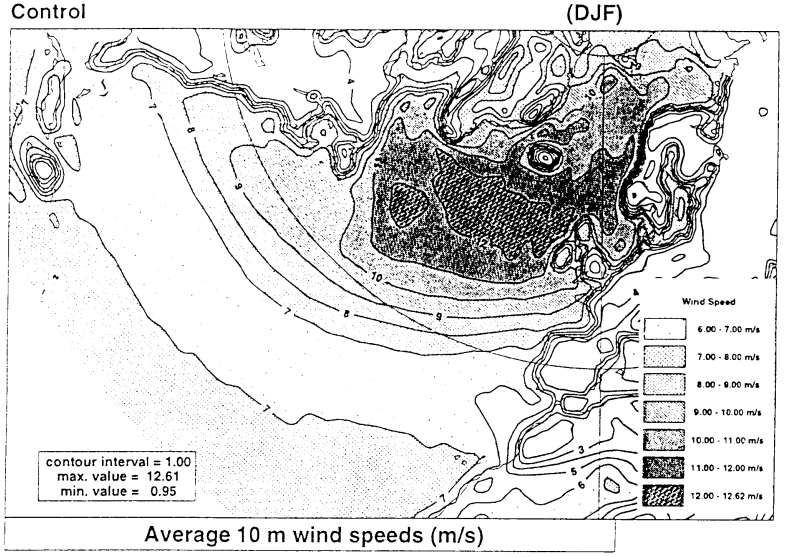

Figure 6.c

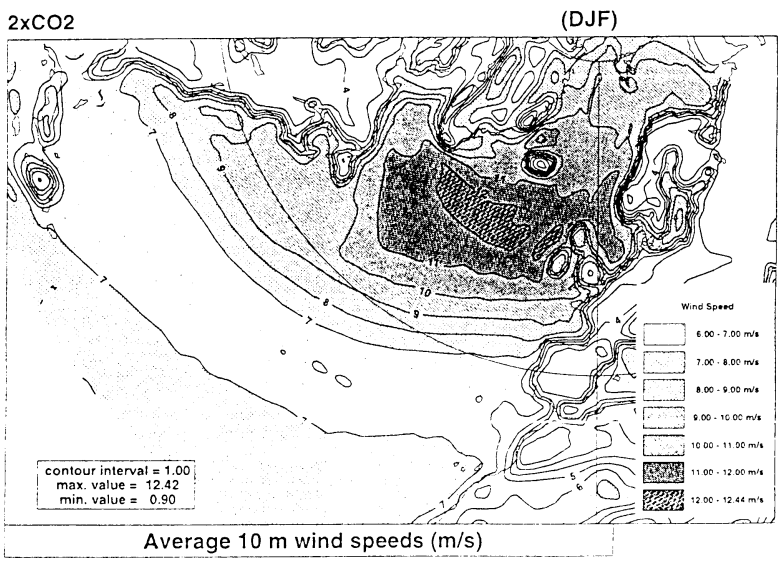

Figure 6.d

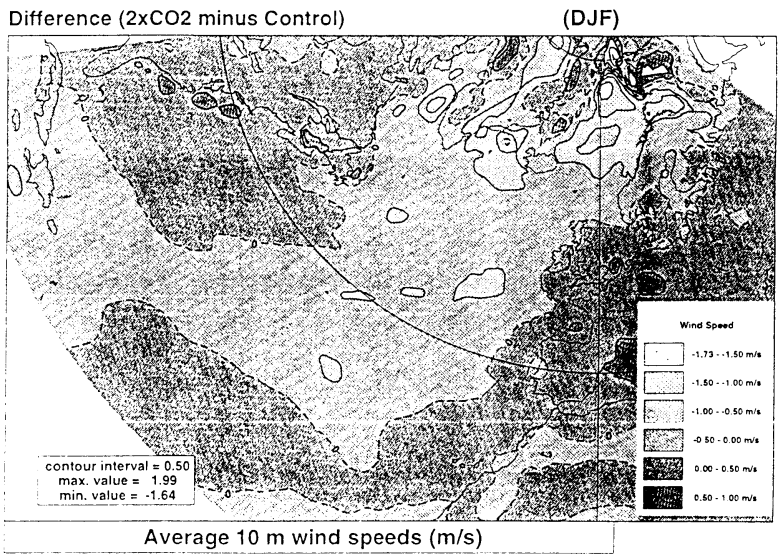

Figure 7.a

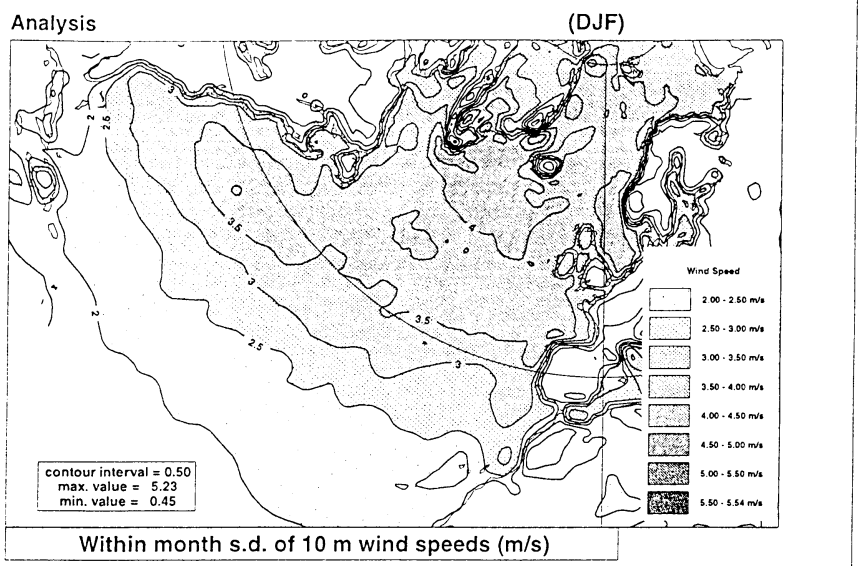

Figure 7.b

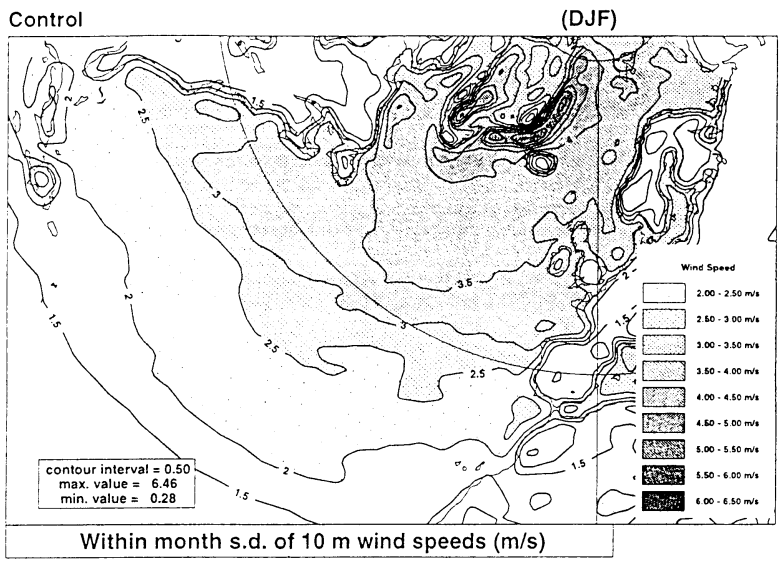

Figure 7.c

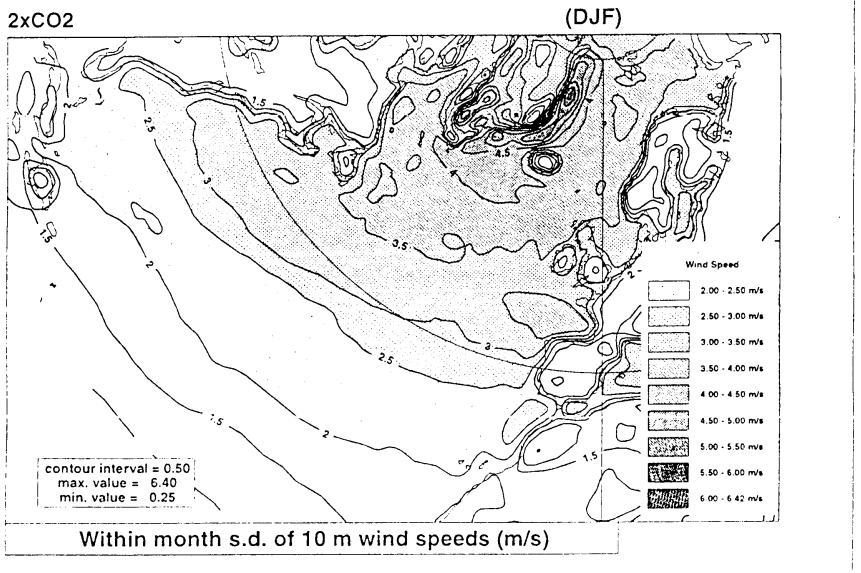

Figure 7.d

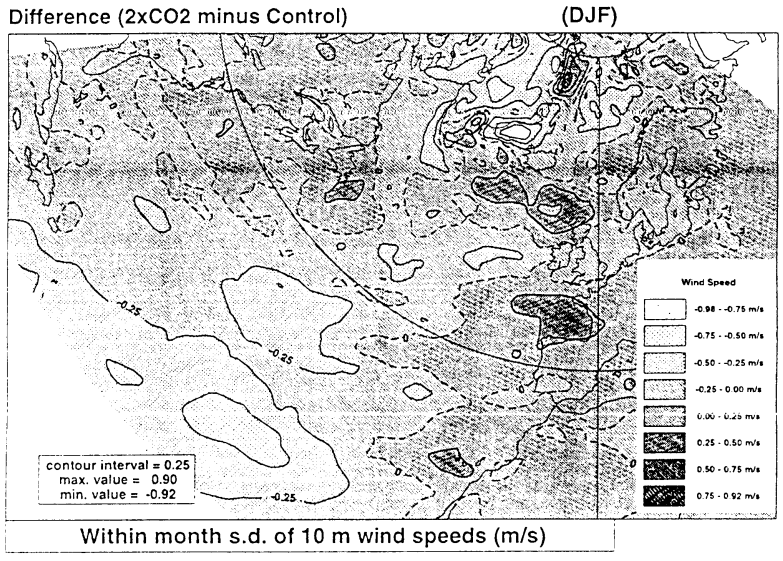

Figure 8.a

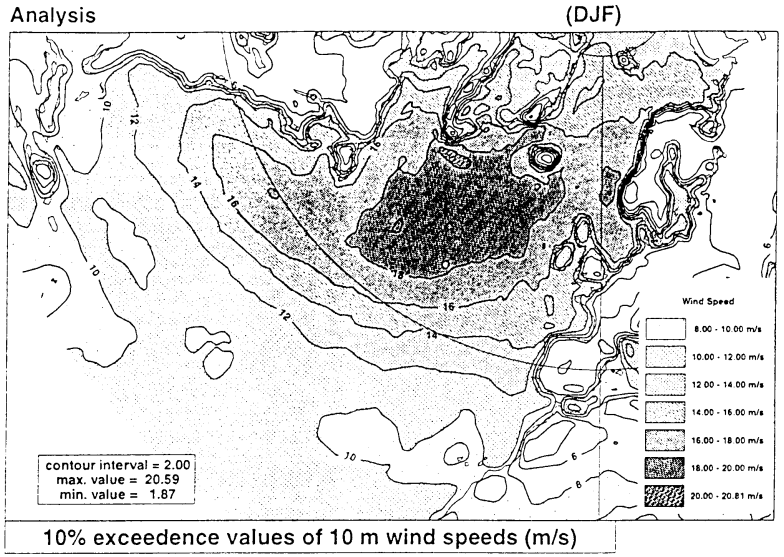

Figure 8.b

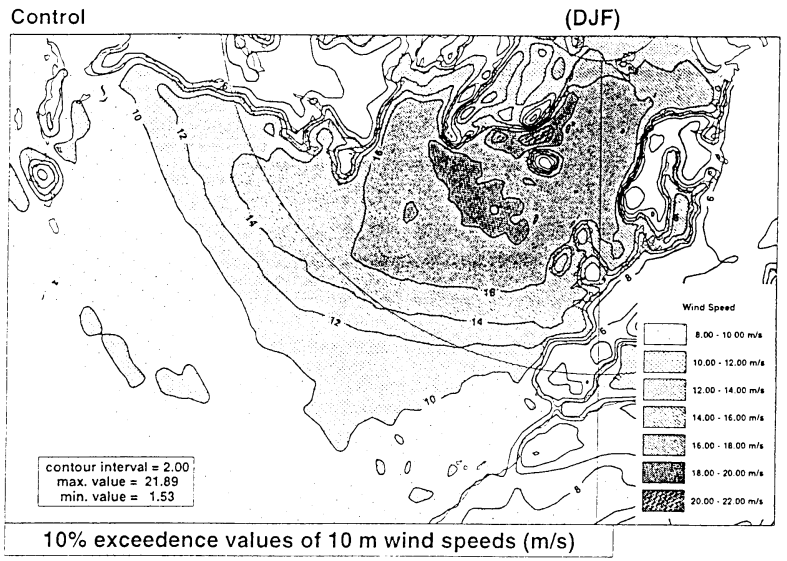

Figure 8.c

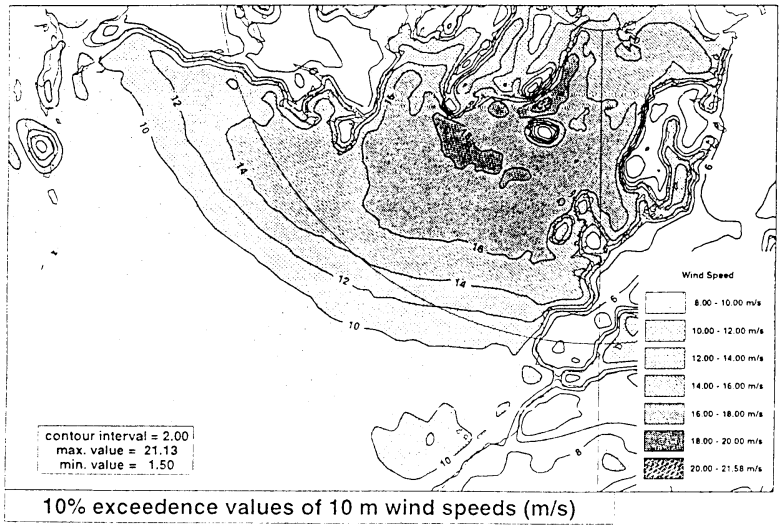

Figure 8.d

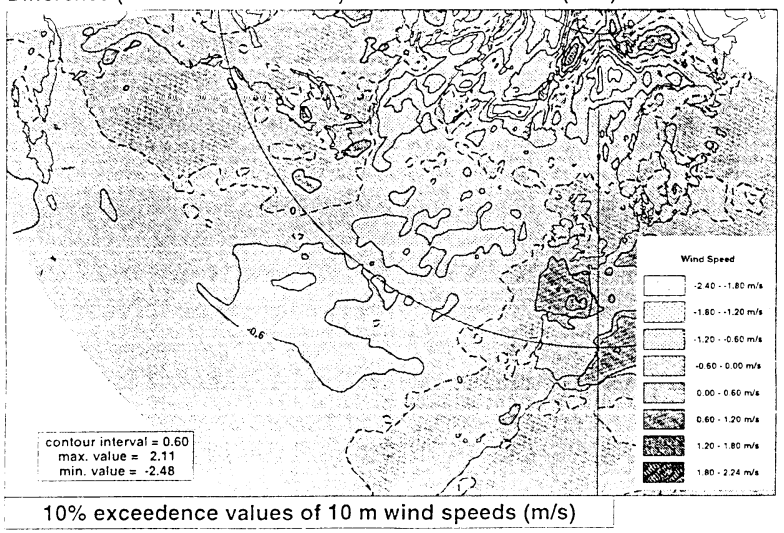

Figure 9.a

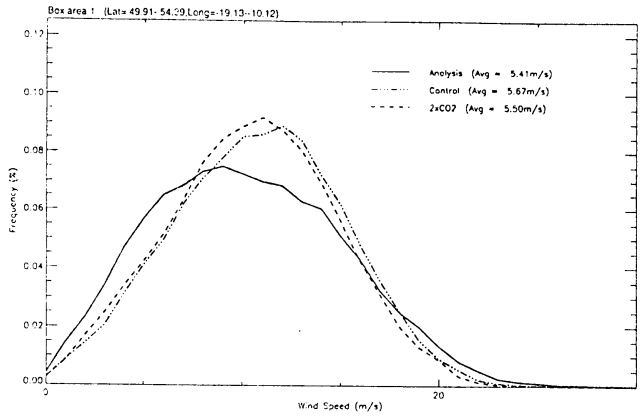

Figure 9.b

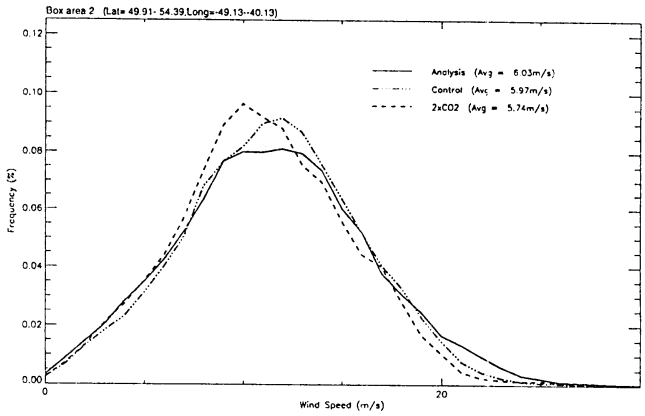

Figure 9.c

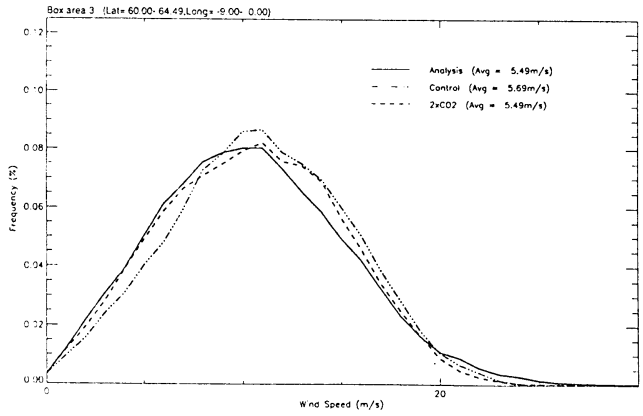

Figure 9.d

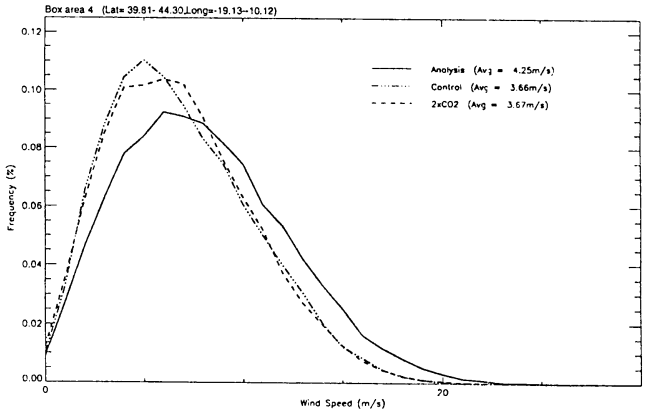

Figure 9.e

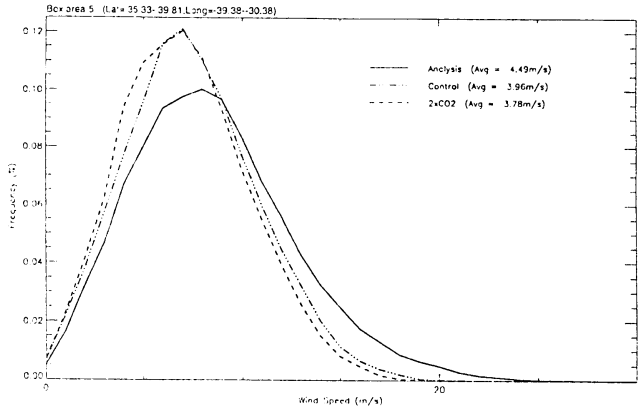

Figure 9.f

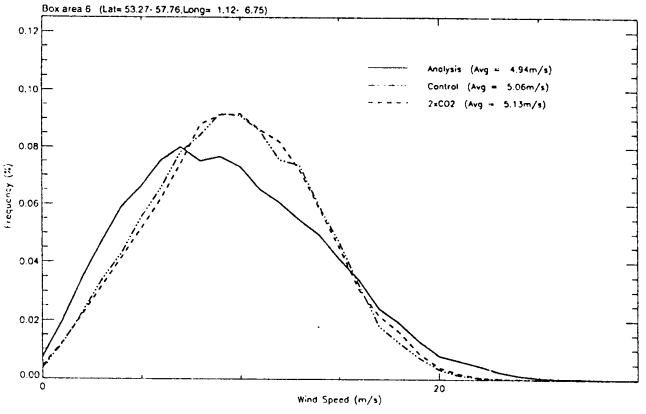

Figure 9: Frequncy distributions (%) of winter (December to February) 10 m wind speeds for 6 box areas in the North Atlantic and North Sea, see figure 4 for locations. Solid line: ECMWF analyses (1991 to 1995); dot-dashed line: the control (5 winters); dashed line: the $2xCO_2$ scenario (5 winters).

Figure 10.a

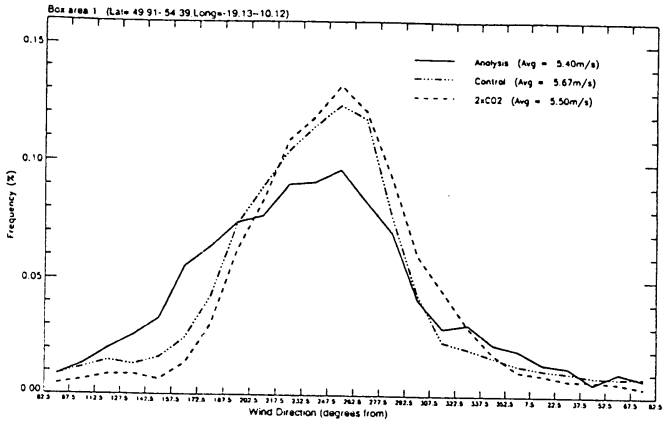

Figure 10.b

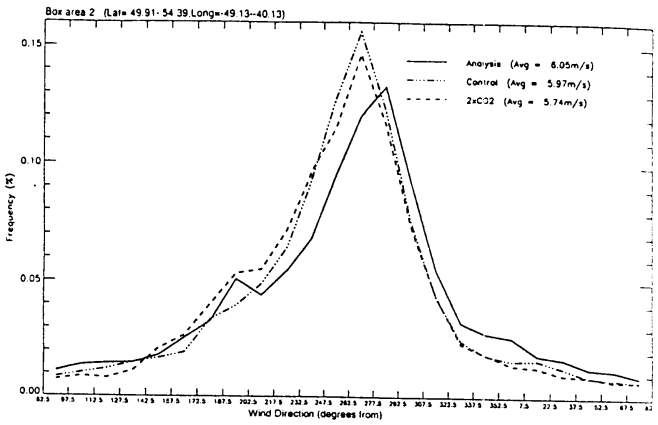

Figure 10.c

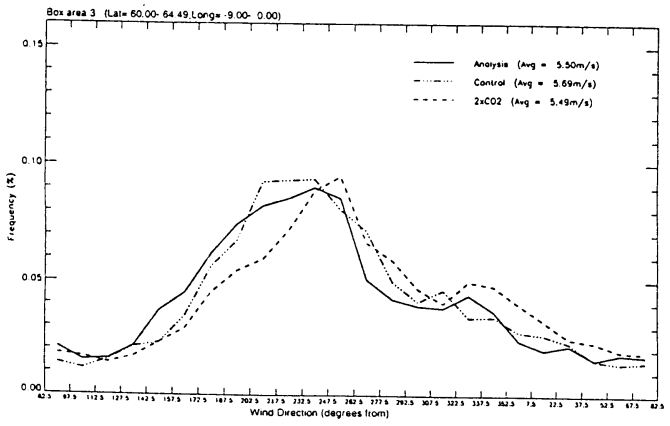

Figure 10.d

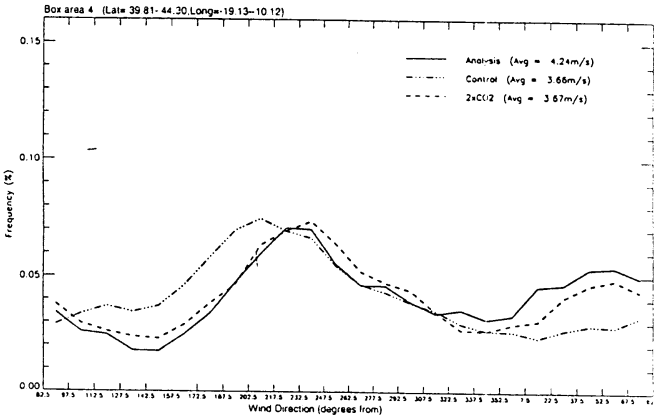

Figure 10.e

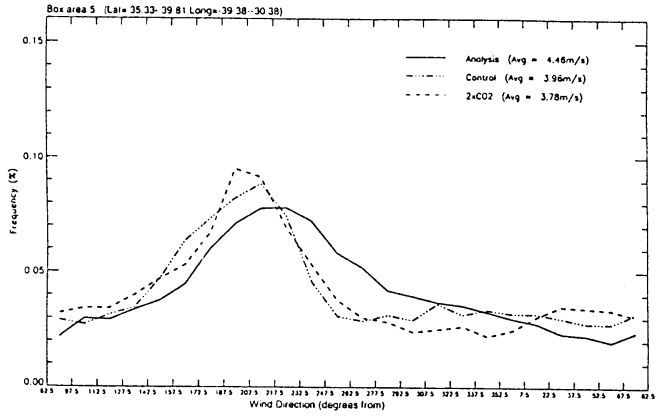

Figure 10.f

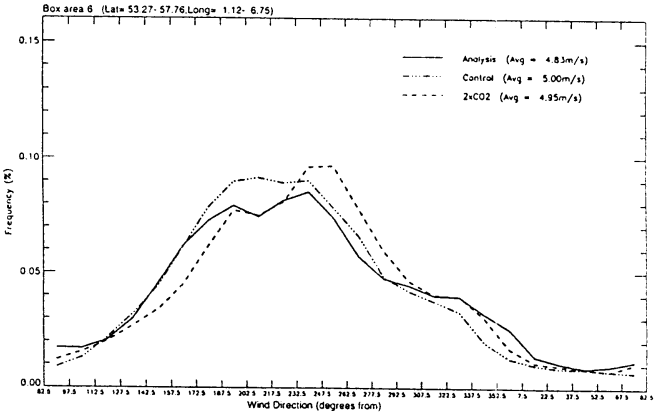

Figure 10: Frequncy distributions (%) of winter (December to February) 10 m wind directions for 6 box areas in the North Atlantic and North Sea, see figure 4 for locations. Solid line: ECMWF analyses (1991 to 1995); dot-dashed line: the control (5 winters); dashed line, the $2xCO_2$ scenario (5 winters)

Figure 11.a

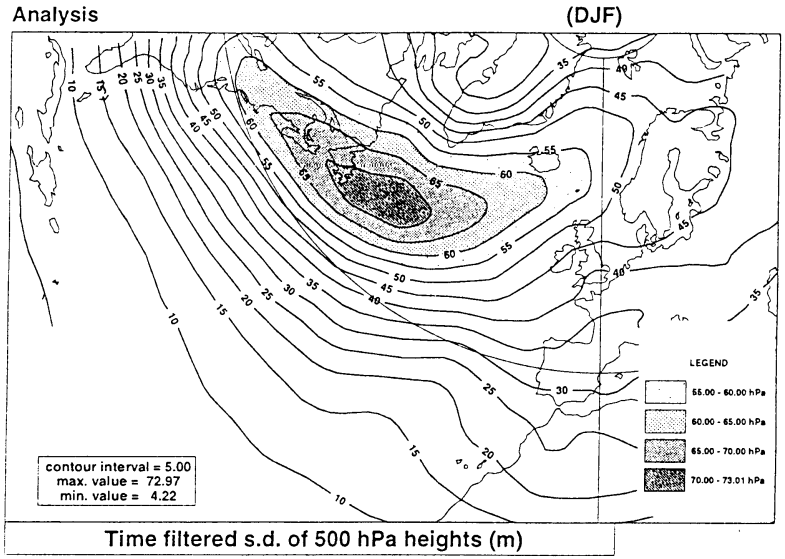

Figure 11.b

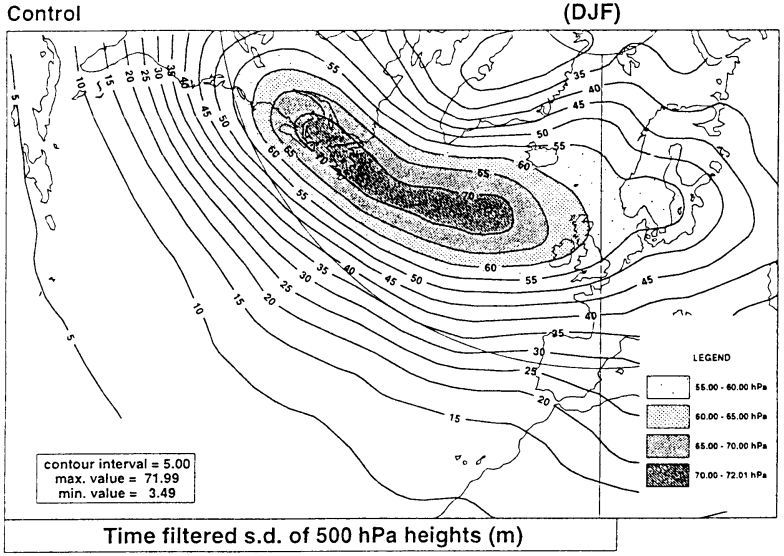

Figure 11.c

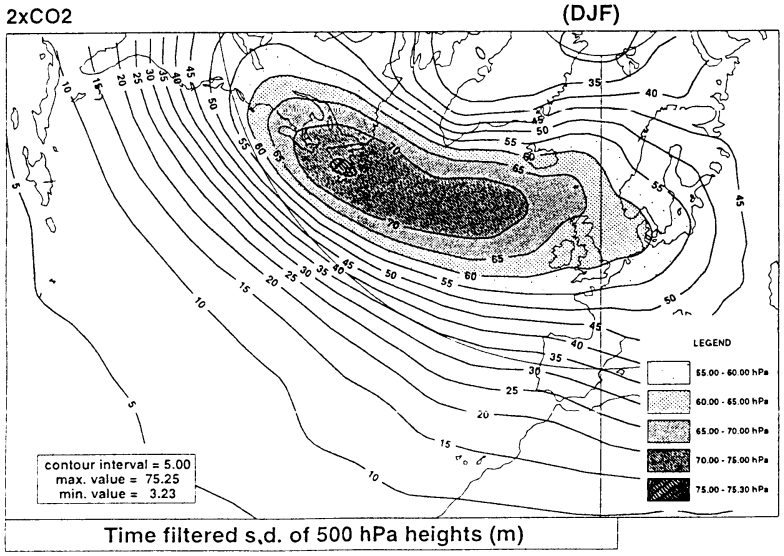

Figure 11: Standard deviation of the band-pass (2.5-6 days) filtered winter (December to February) 500 hPa heights over the North Atlantic area for a) the ECMWF analyses (1991 to 1995), b) the control (6 winters) and c) the $2xCO_2$ scenario (6 winters).

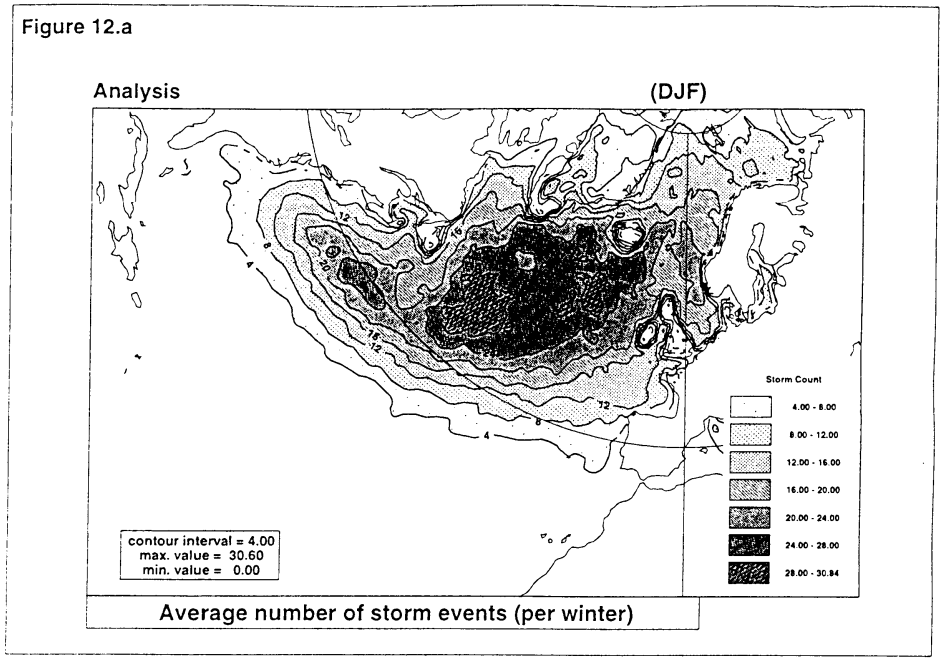

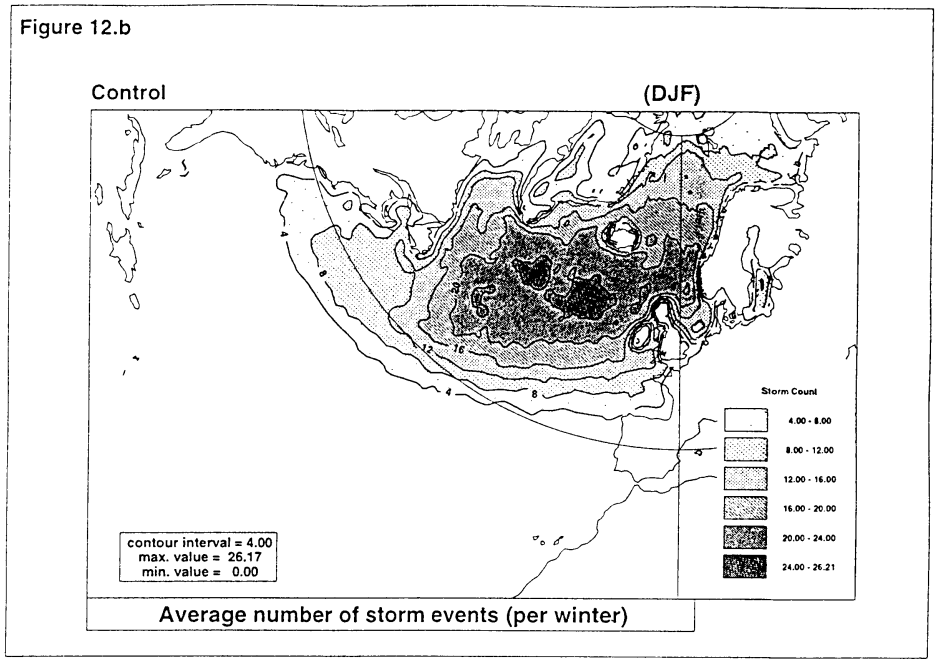

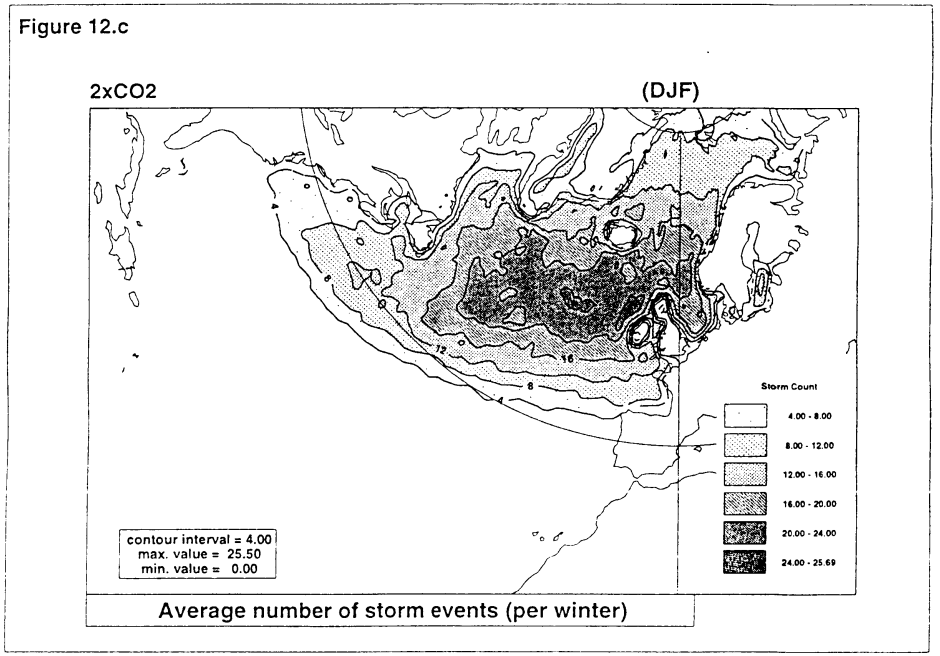

Figure 12: Number of storm events per winter (December to February) over the North Atlantic area for a) the ECMWF analyses (1991 to 1995), b) the control (6 winters) and c) the $2xCO_2$ scenario (6 winters). See text for further details.

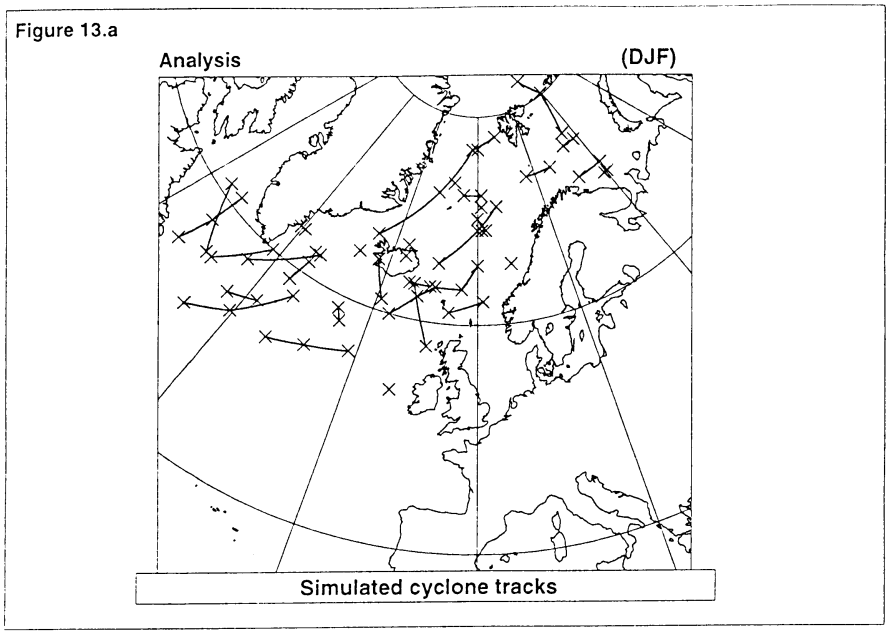

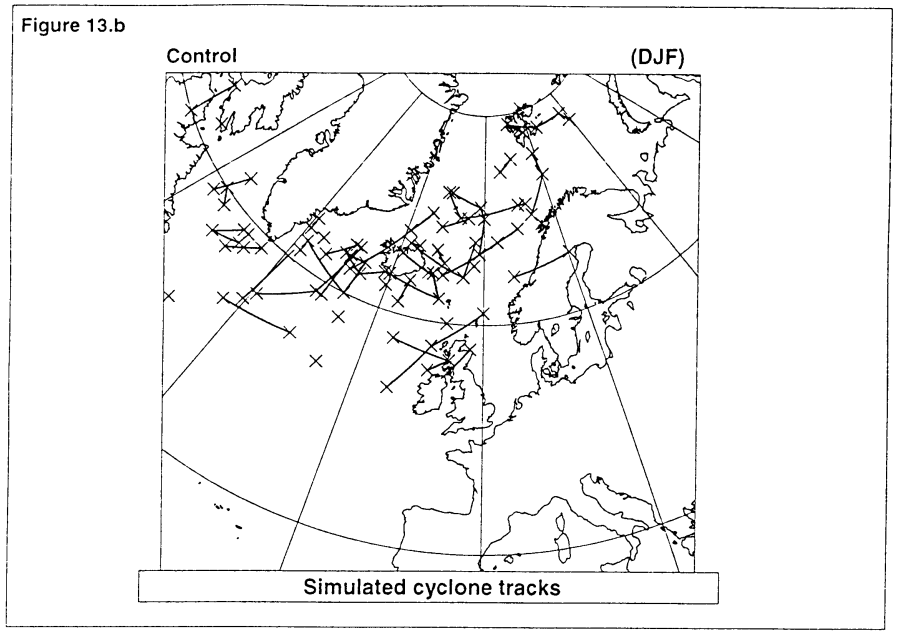

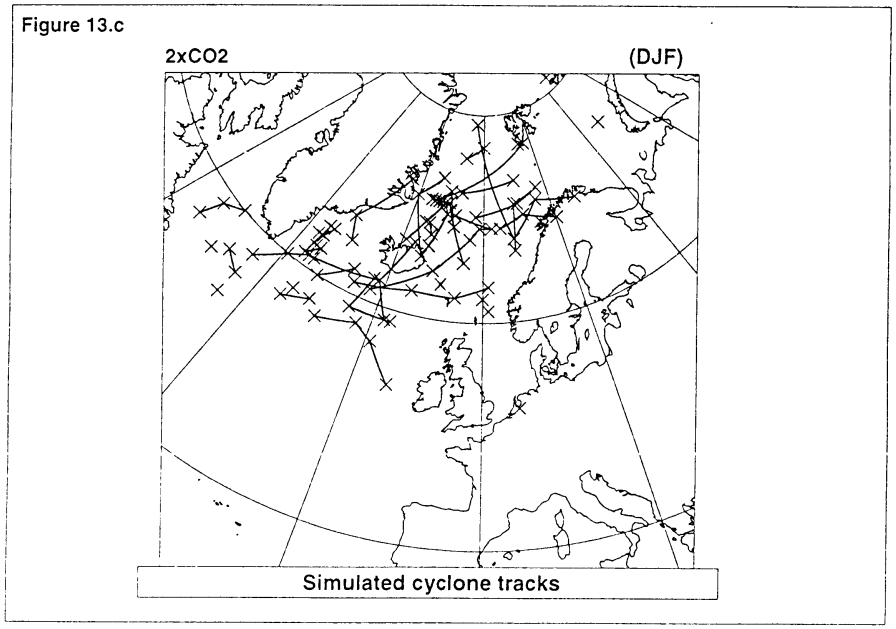

Figure 13: Tracks of cyclones with core pressure < 950 hPa in the North Atlantic area for a) the ECMWF analyses (1991 to 1995) (30 independent storms), b) the control (5 winters) (41 independent storms) and c) the $2xCO_2$ scenario (5 winters) (36 independent storms).

Figure 14.a

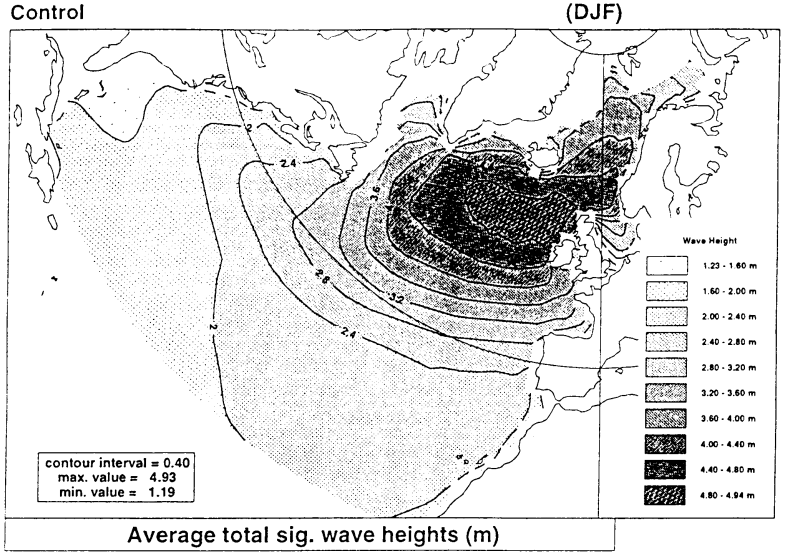

Figure 14.b

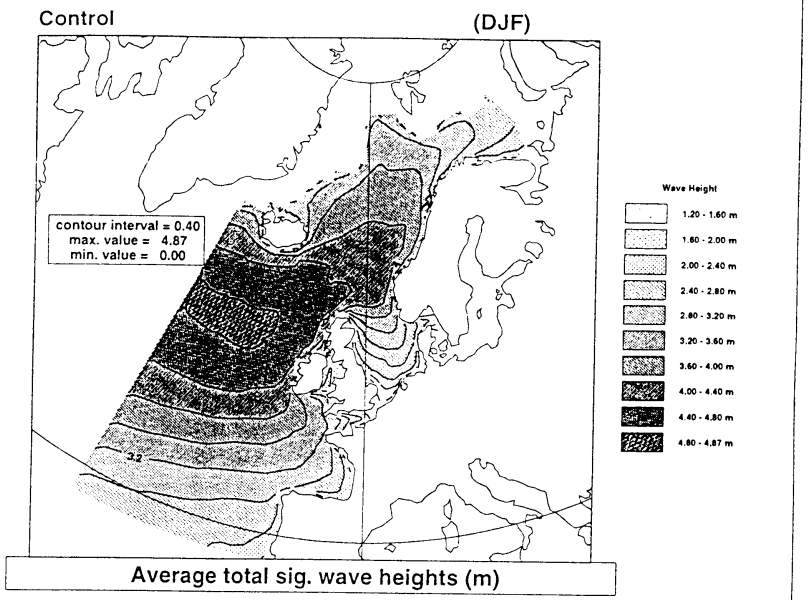

Figure 14.c

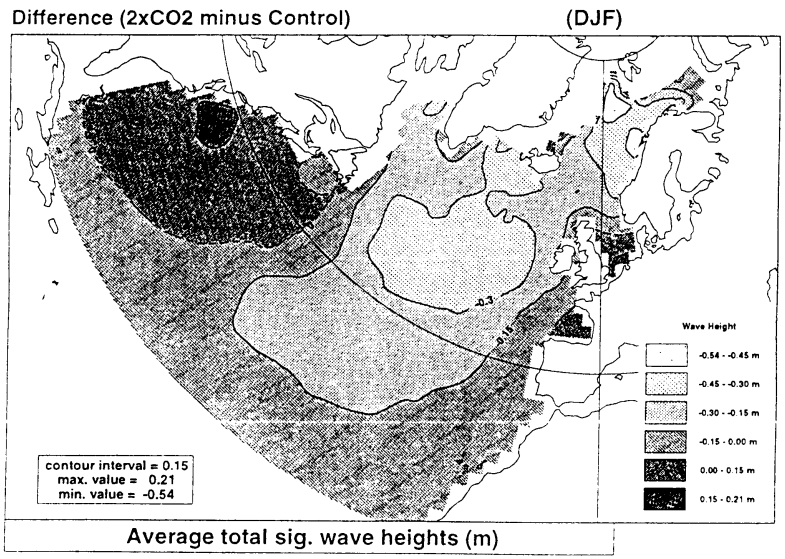

Figure 14.d

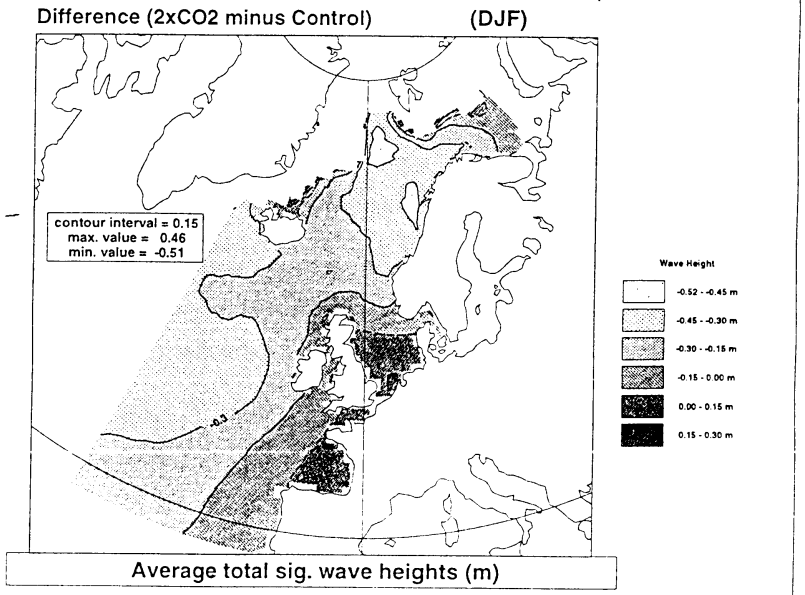

Figure 15 a)

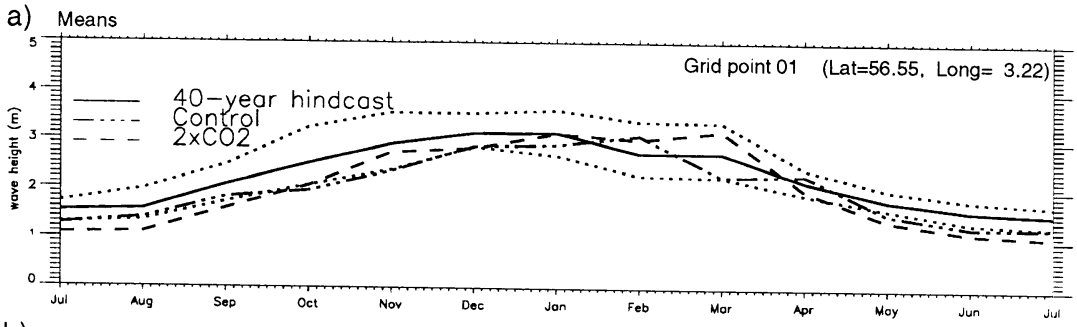

b)

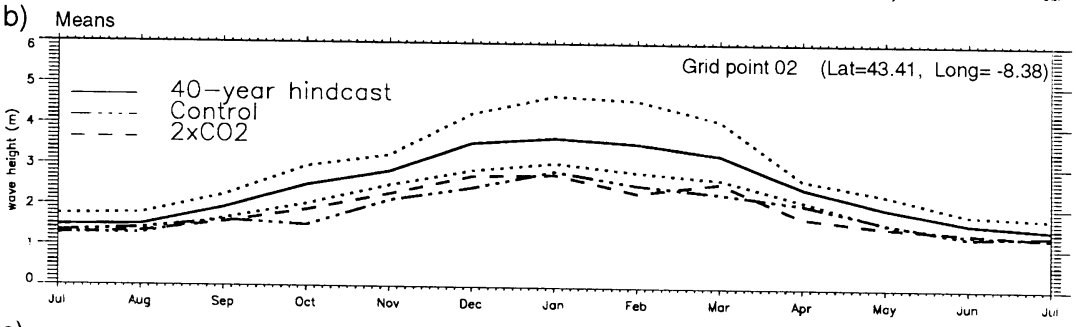

c)

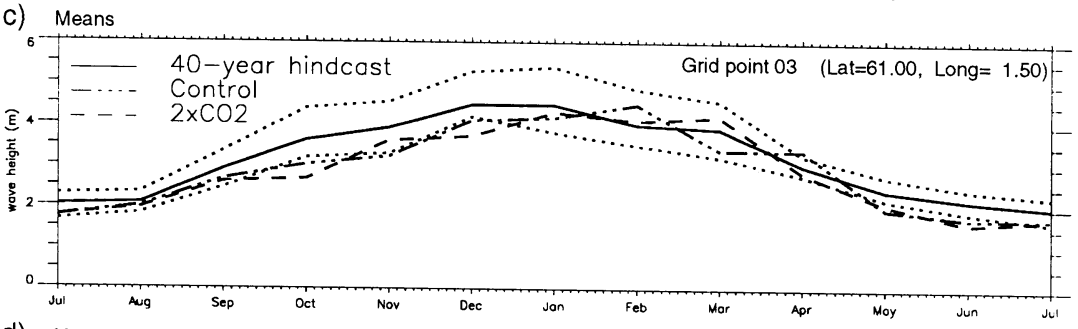

d)

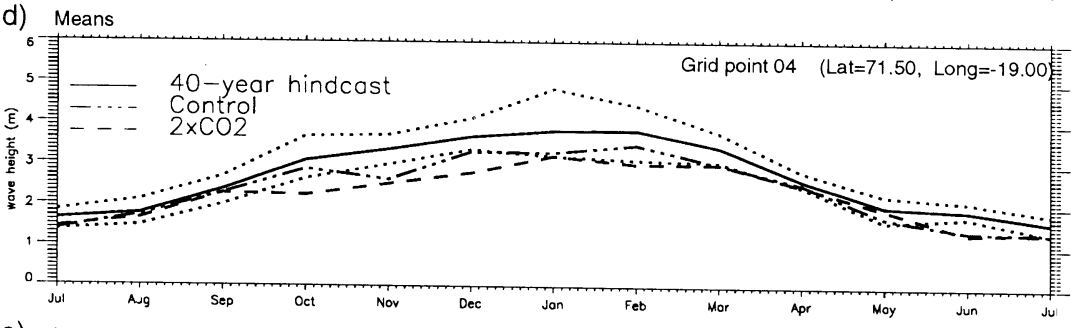

e)

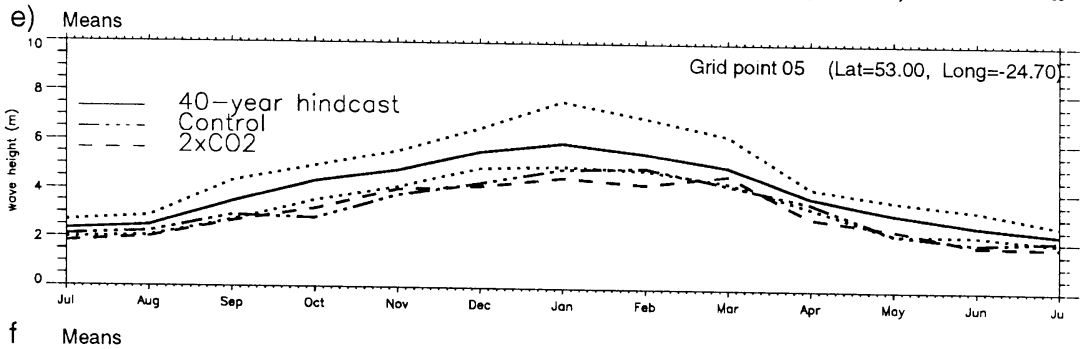

f

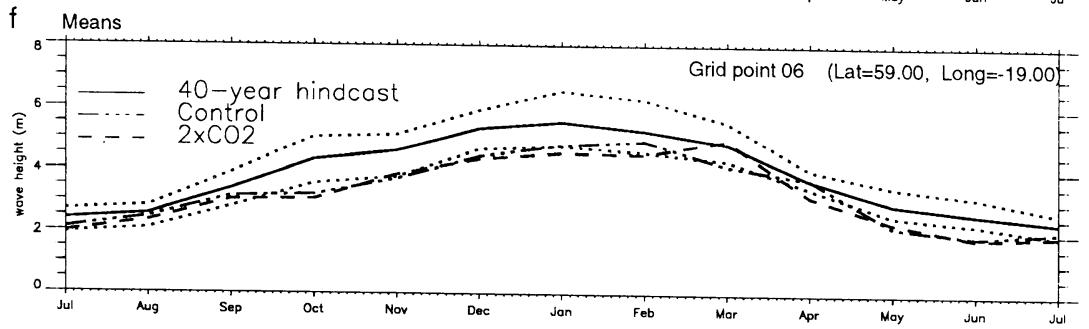

Figure 16 a)

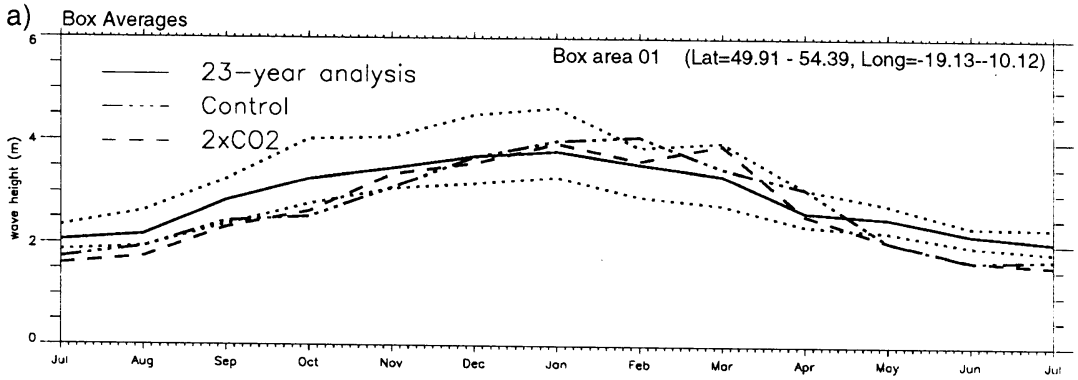

b)

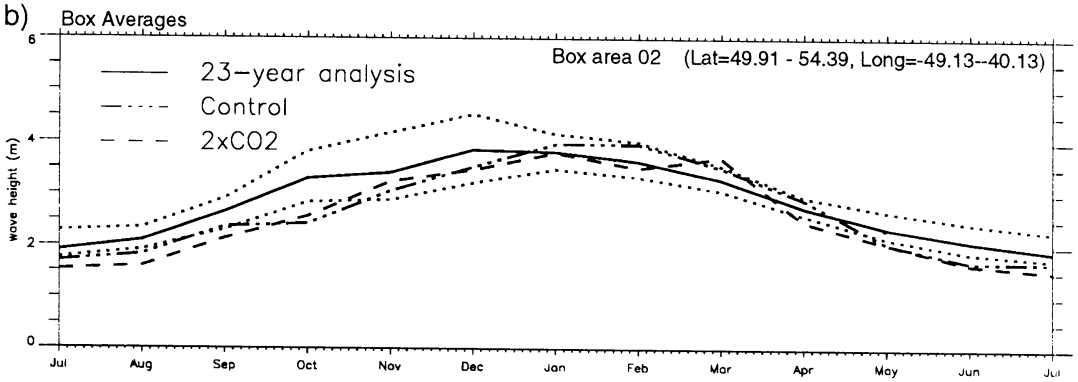

c)

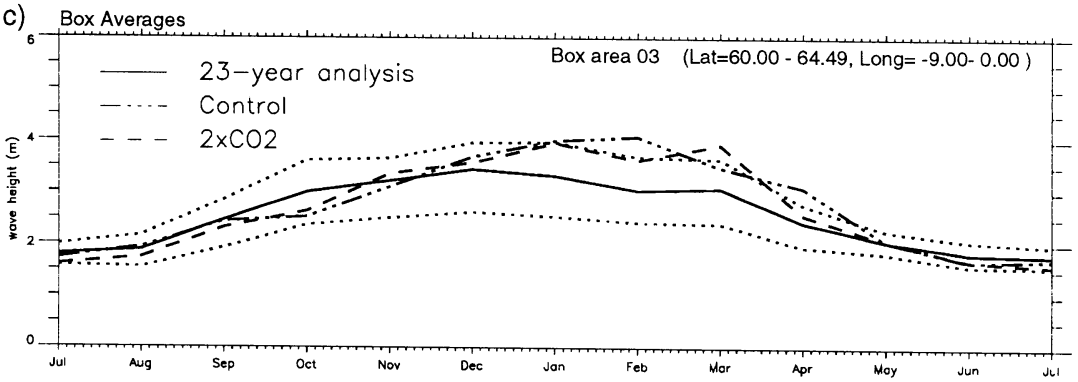

d)

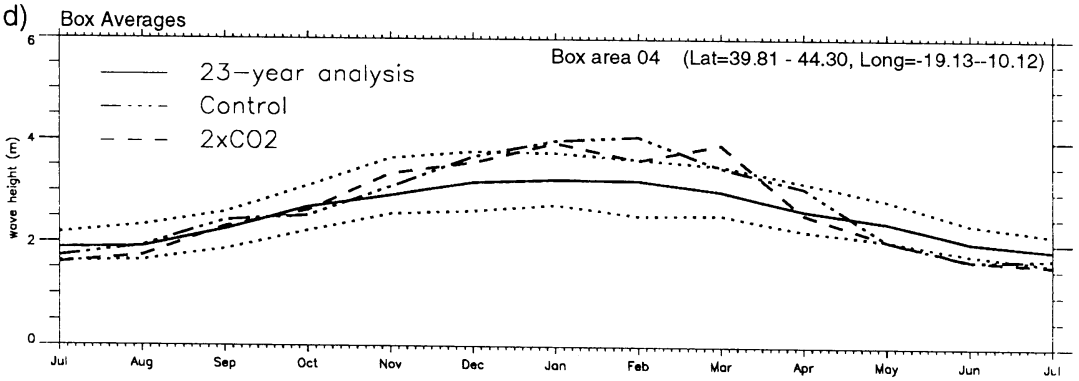

e)

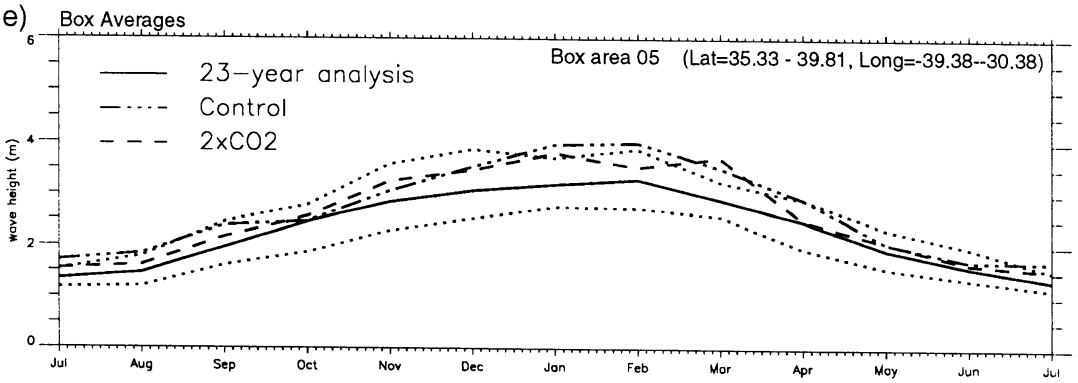

Figure 17.a

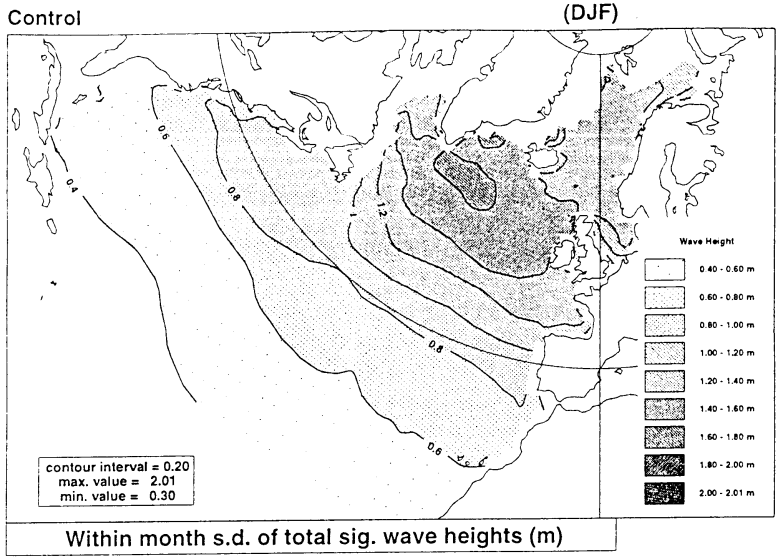

Figure 17.b

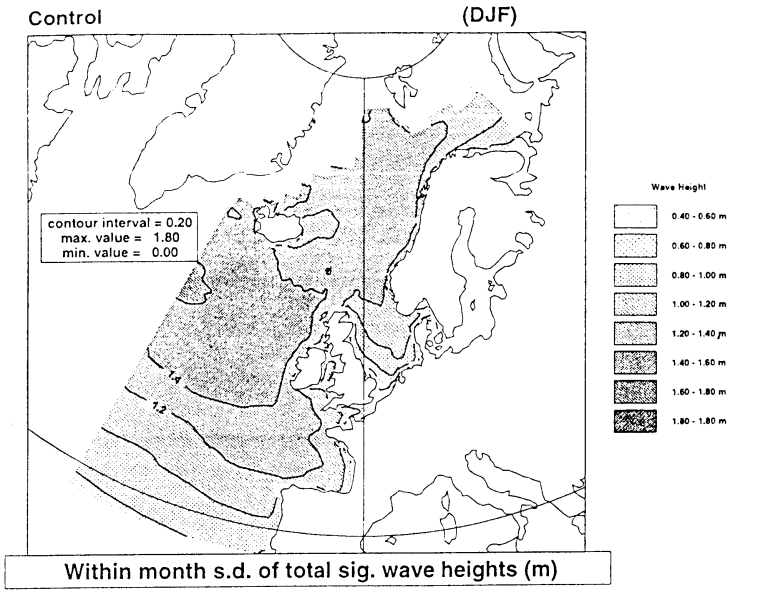

Figure 17.c

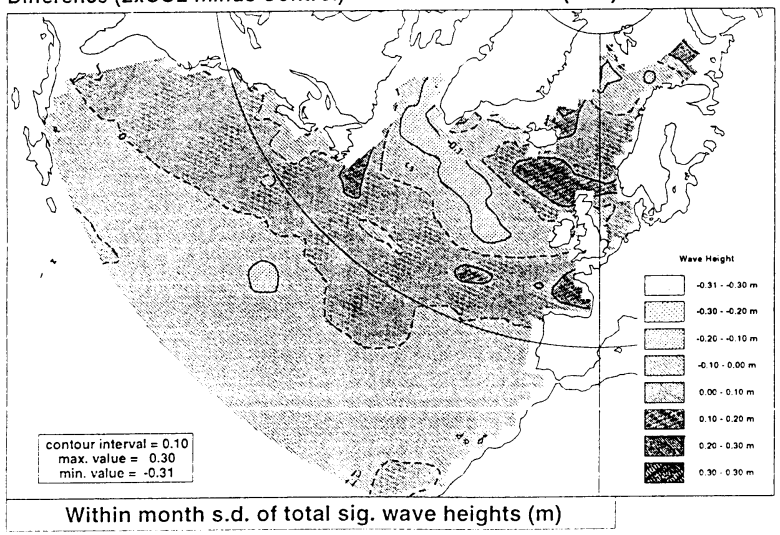

Figure 17.d

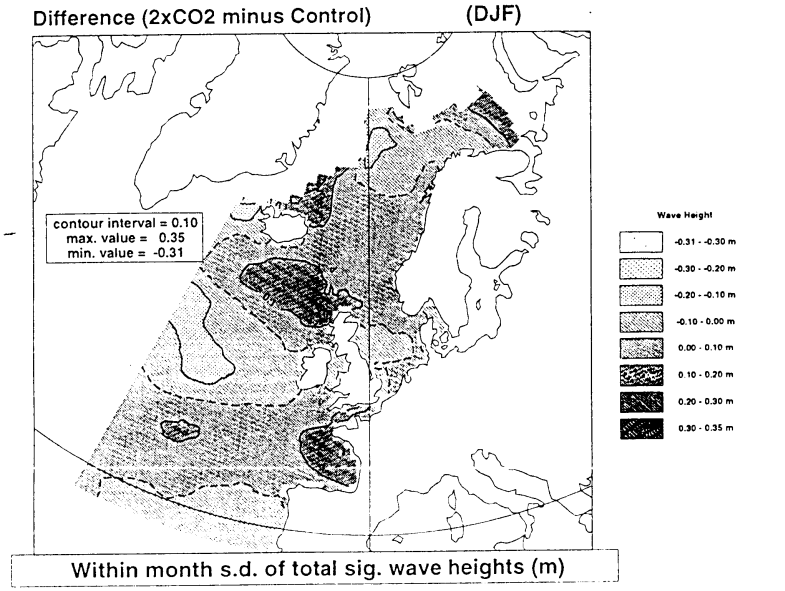

Figure 18.a

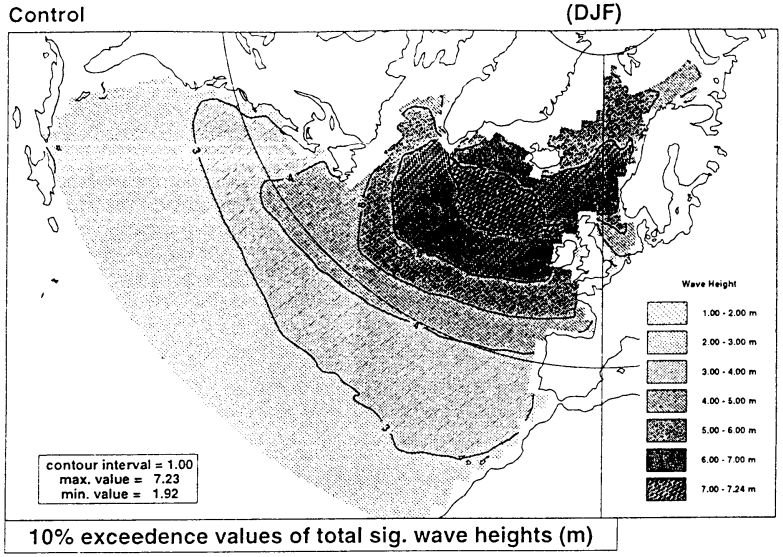

10% exceedence values of total sig. wave heights (m)

Figure 18.b

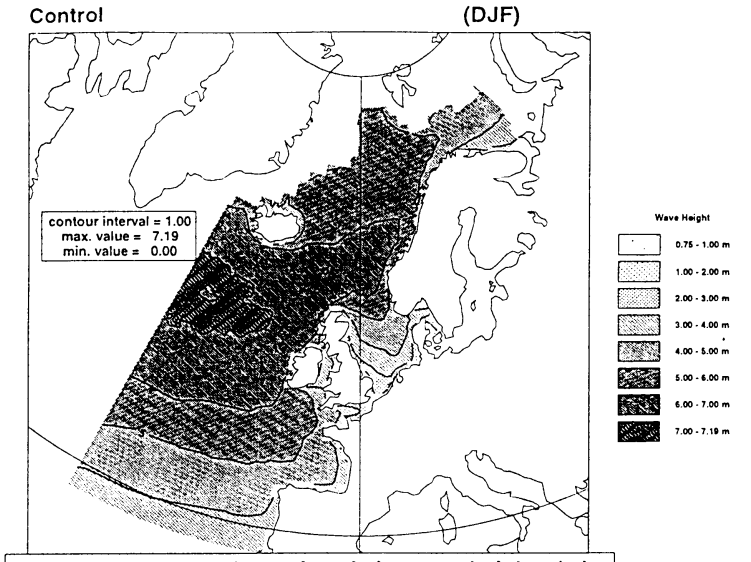

10% exceedence values of total sig. wave heights (m)

Figure 18.c

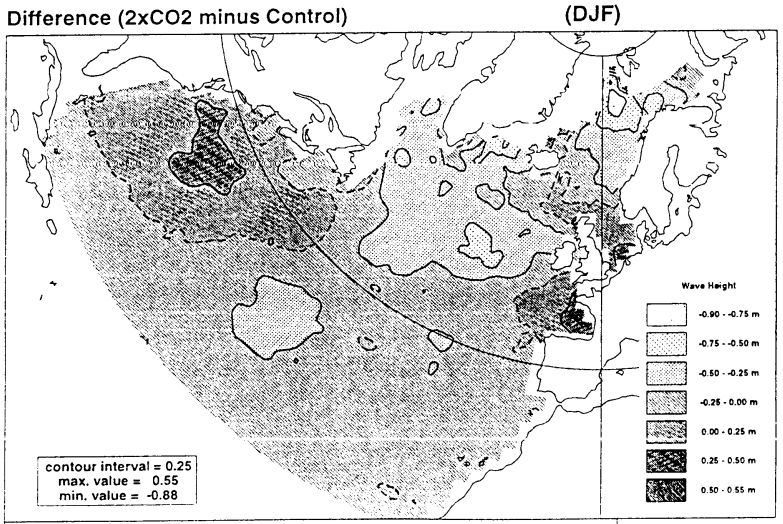

10% exceedence values of total sig. wave heights (m)

Figure 18.d

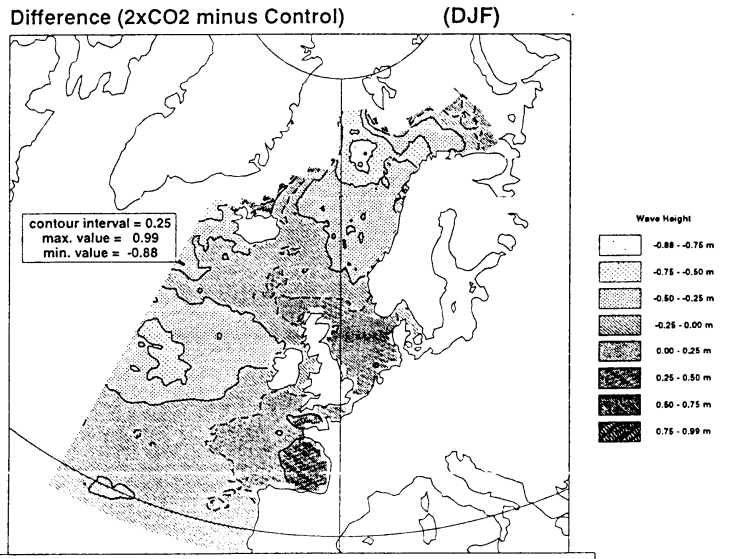

10% exceedence values of total sig. wave heights (m)

Figure 19 a)

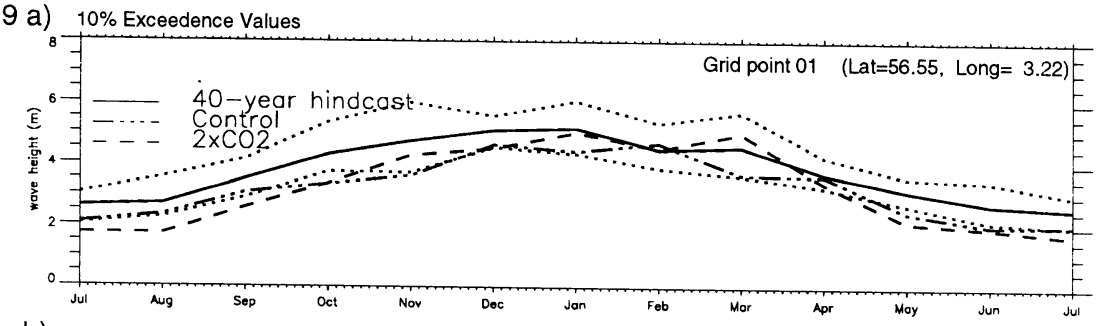

b)

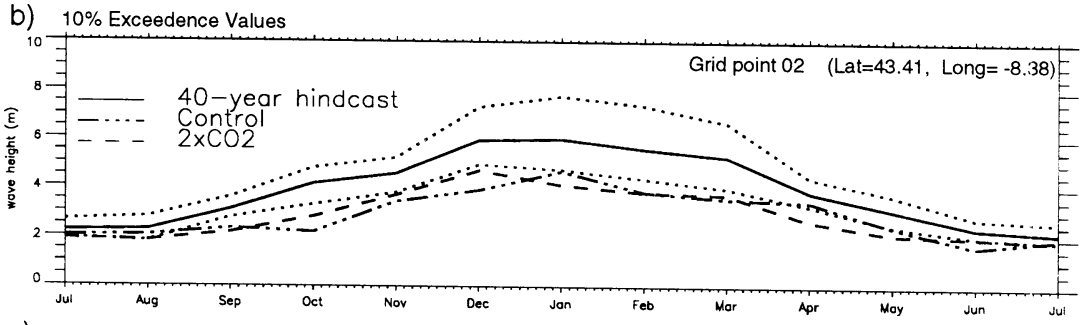

c)

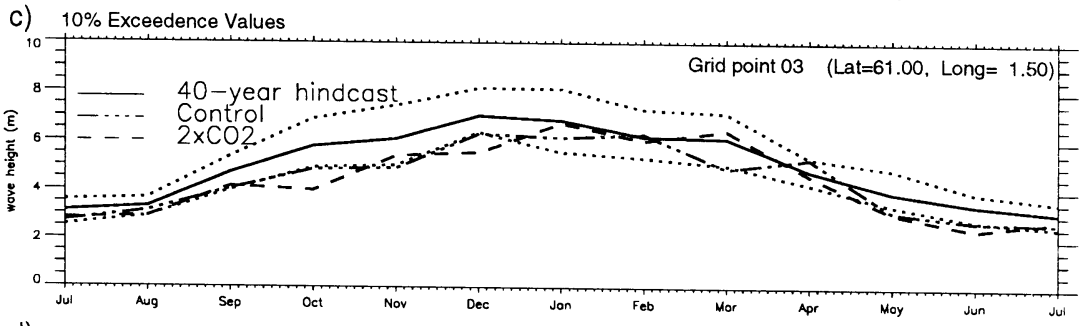

d)

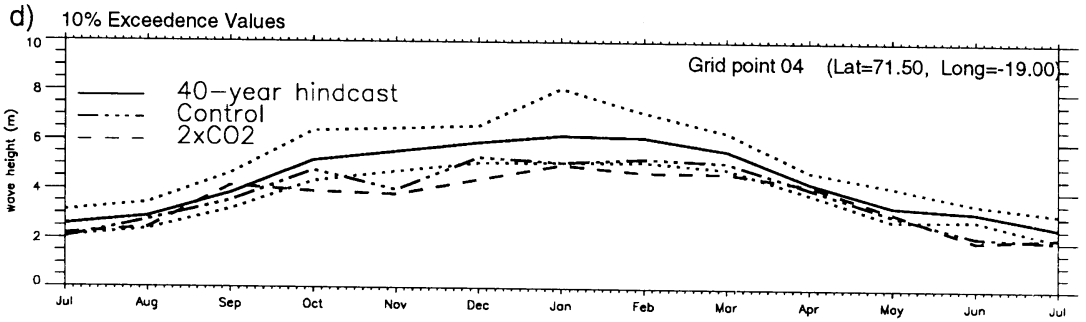

e)

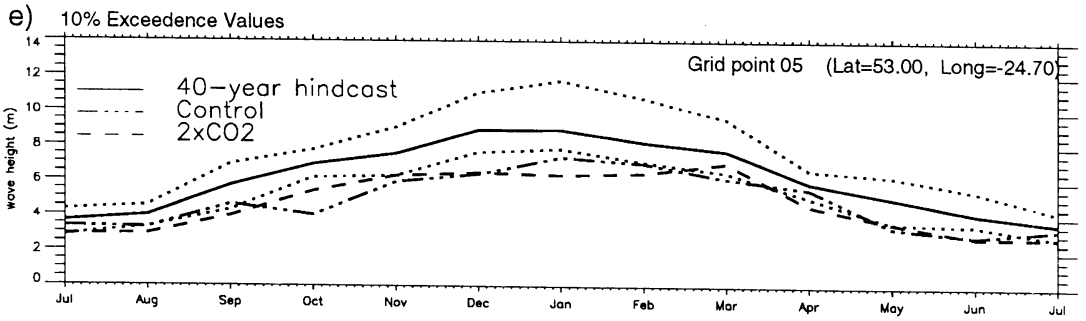

f

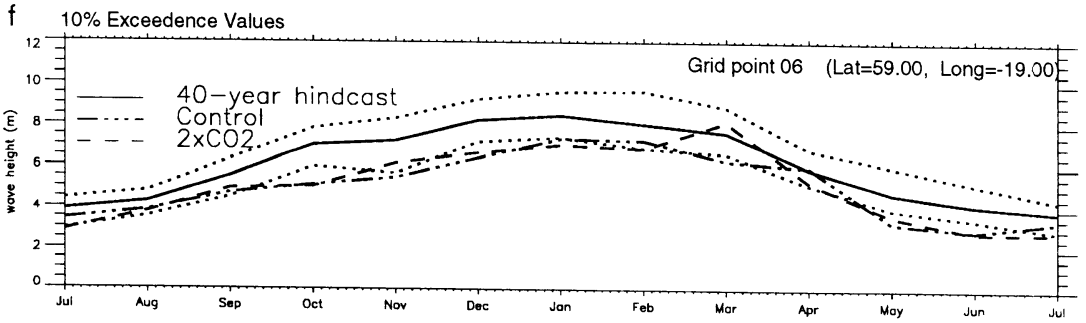

Figure 20 a)

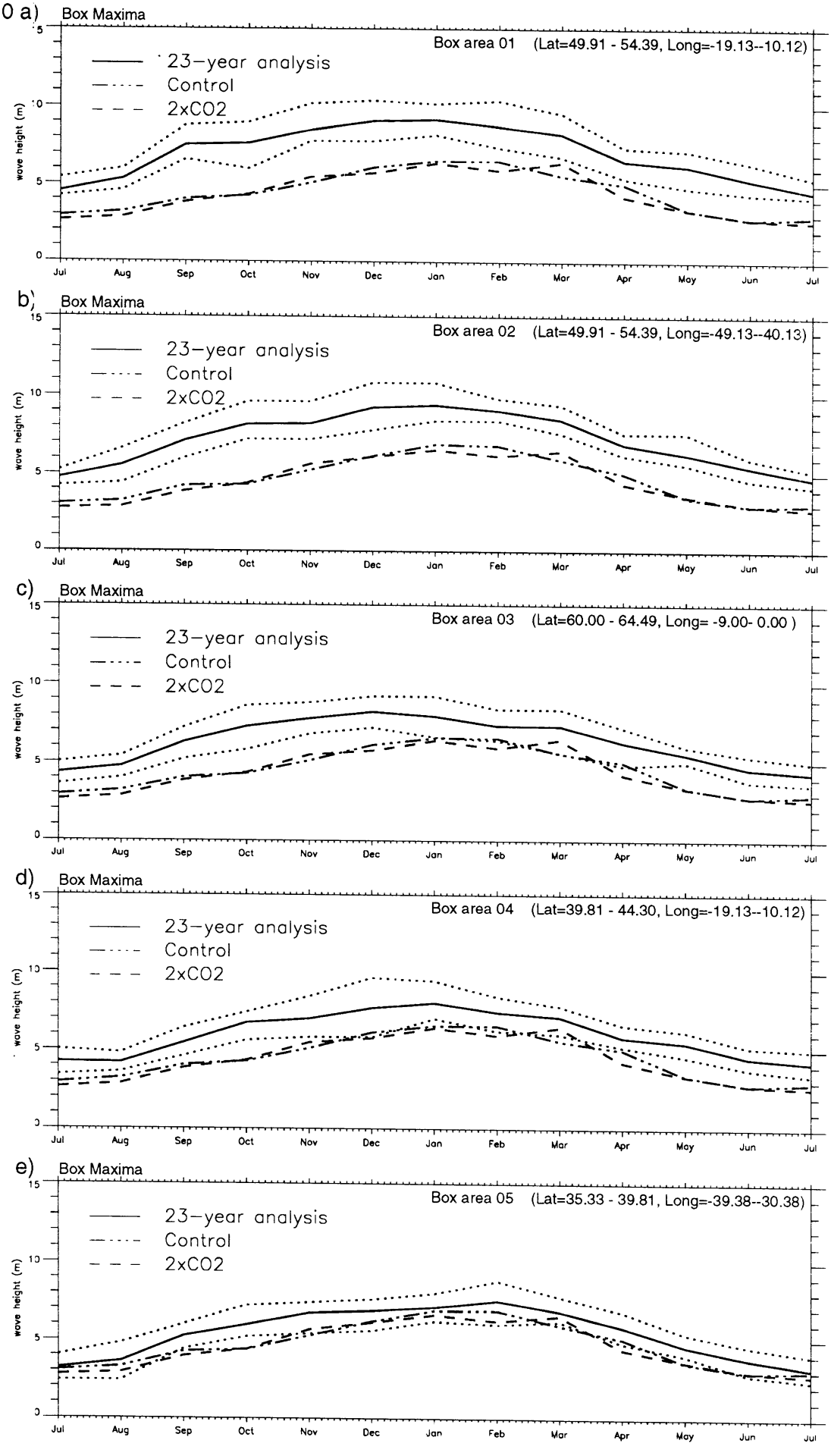
Box Maxima
Box area 01 (Lat=49.91 - 54.39, Long=-19.13--10.12)
23-year analysis
Control
2xCO2
wave height (m)
Jul Aug Sep Oct Nov Dec Jan Feb Mar Apr May Jun Jul
b)
Box Maxima
Box area 02 (Lat=49.91 - 54.39, Long=-49.13--40.13)
23-year analysis
Control
2xCO2
wave height (m)
Jul Aug Sep Oct Nov Dec Jan Feb Mar Apr May Jun Jul
c)
Box Maxima
Box area 03 (Lat=60.00 - 64.49, Long= -9.00- 0.00)
23-year analysis
Control
2xCO2
wave height (m)
Jul Aug Sep Oct Nov Dec Jan Feb Mar Apr May Jun Jul
d)
Box Maxima
Box area 04 (Lat=39.81 - 44.30, Long=-19.13--10.12)
23-year analysis
Control
2xCO2
wave height (m)
Jul Aug Sep Oct Nov Dec Jan Feb Mar Apr May Jun Jul
e)
Box Maxima
Box area 05 (Lat=35.33 - 39.81, Long=-39.38--30.38)
23-year analysis
Control
2xCO2
wave height (m)
Jul Aug Sep Oct Nov Dec Jan Feb Mar Apr May Jun Jul

Figure 21 a)

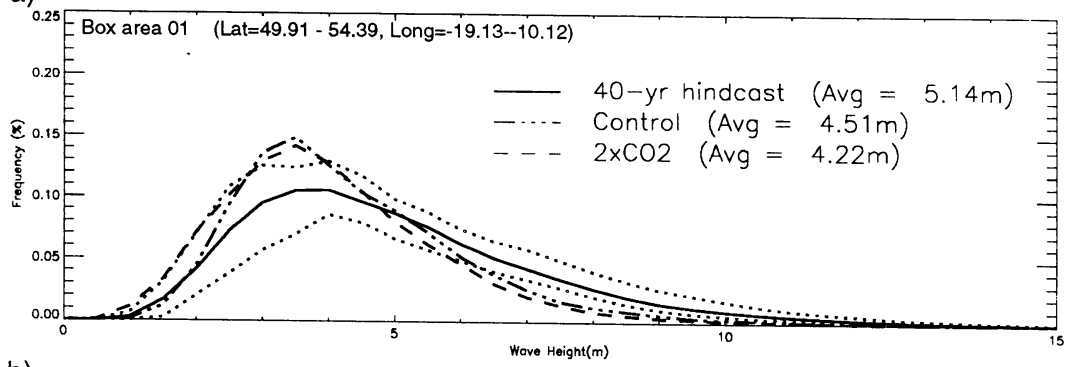

b)

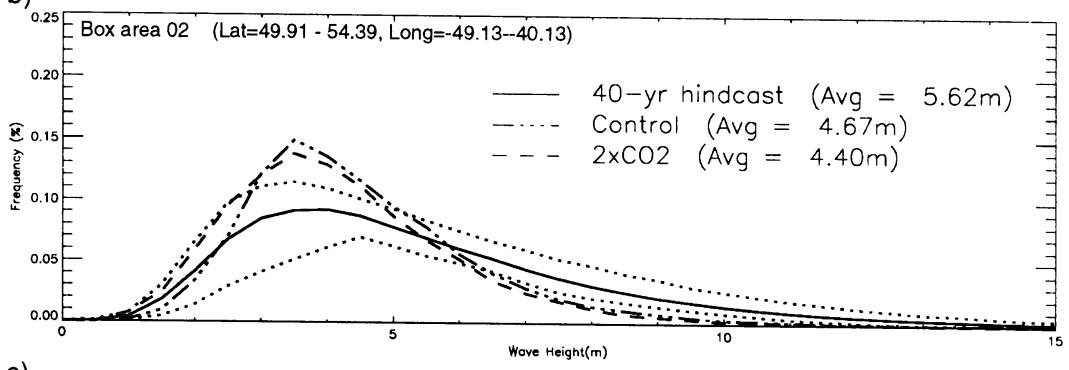

c)

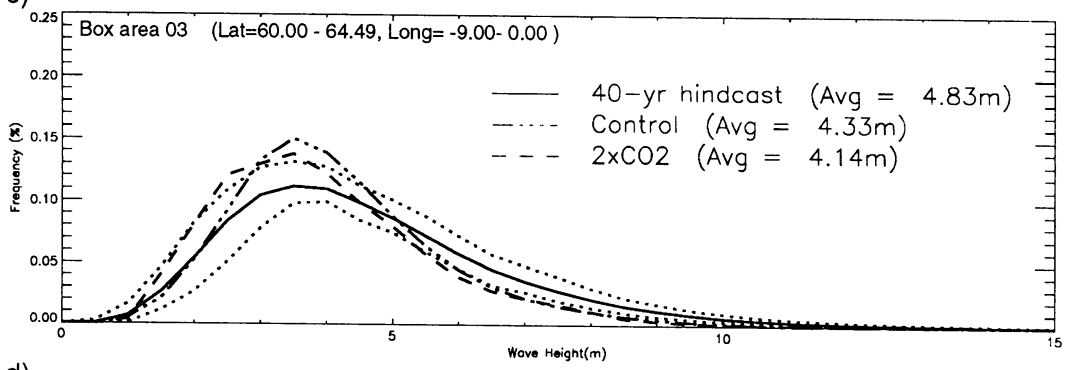

d)

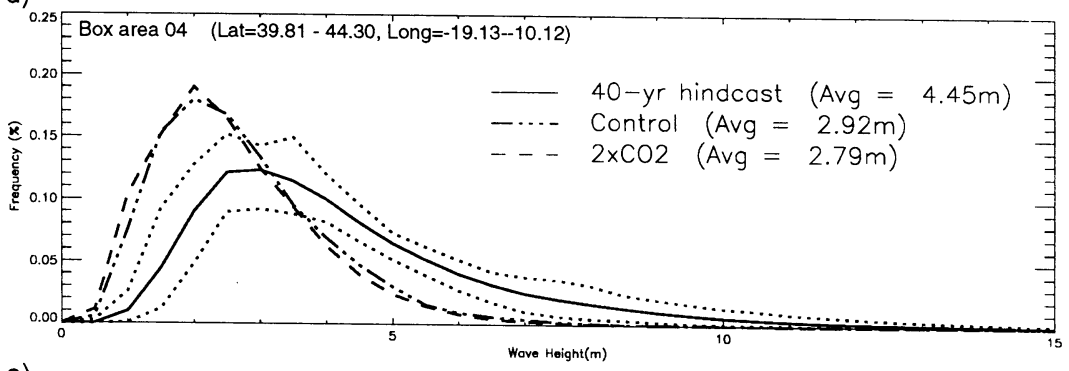

e)

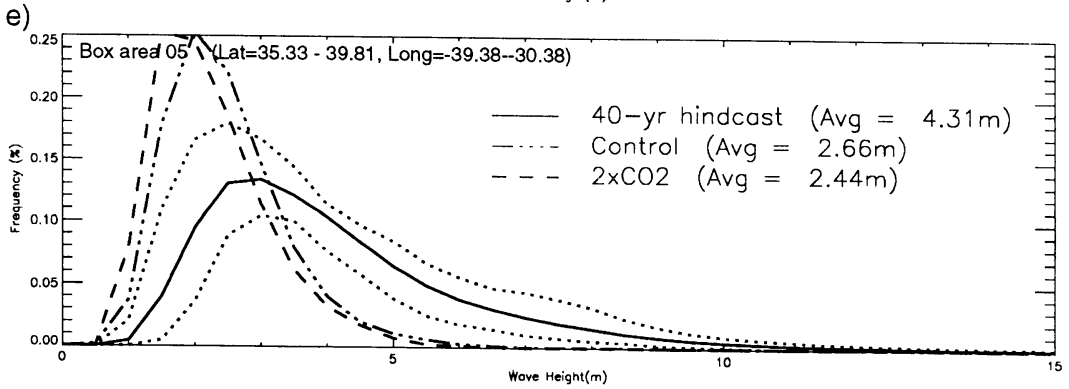

Figure 22.a

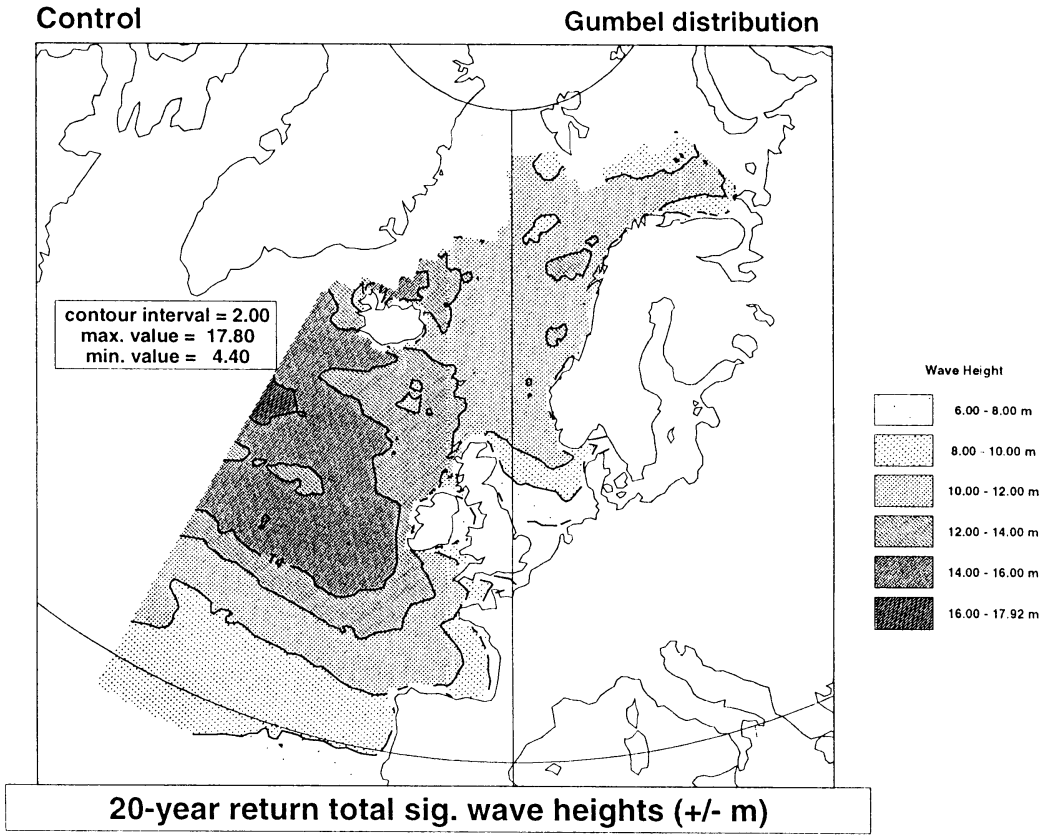

Figure 22.b

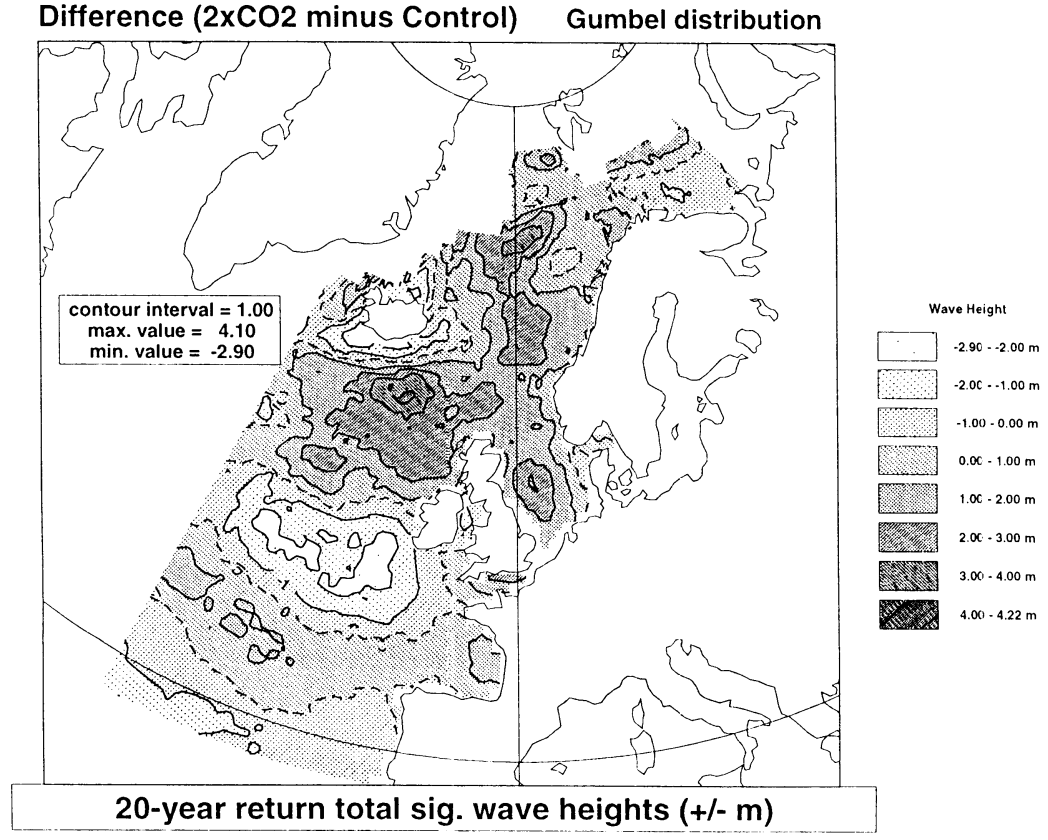

Figure 23.a

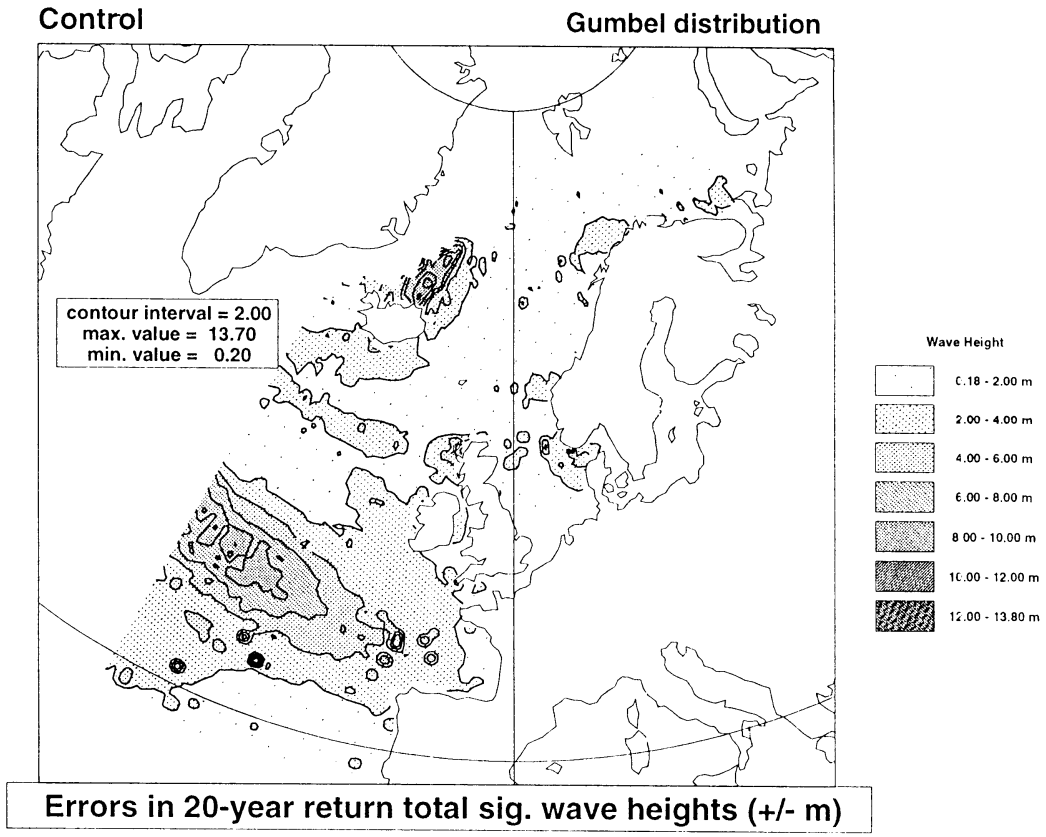

Figure 23.b